

MOLECULAR SIEVE ZEOLITIC-IMIDAZOLATE FRAMEWORK ZIF-90 THIN FILMS
AND MEMBRANES FOR GAS SEPARATION APPLICATIONS

A Thesis

by

YU-CHEN HSU

Submitted to the Office of Graduate and Professional Studies of
Texas A&M University
in partial fulfillment of the requirements for the degree of

MASTER OF SCIENCE

Chair of Committee,	Hae-Kwon Jeong
Committee Members,	Hongcai Zhou
	Mustafa Akbulut
Head of Department,	M. Nazmul Karim

May 2018

Major Subject: Chemical Engineering

Copyright 2018 Yu Chen Hsu

ABSTRACT

Hydrocarbon separation in the industry is challenging and currently achieved by well-established relative energy intensive and multi-column distillation processes. Even if many promising membrane-based separation technologies were developed to deal with the issues in hydrocarbon separations, we could find limited practical applications by polymeric membranes because of low selectivity and stability in separation process of industry.

Zeolitic-imidazolate frameworks (ZIFs) have large potential owing to their well-defined aperture size, robustness, and excellent thermal/chemical stability. Recently, ZIF-90 membranes with effective aperture size ~ 5.0 Å have been investigated to have a large potential to separate C4 hydrocarbons such as n-butane/i-butane mixture which cannot be effectively separated by ZIF-8 membranes. However, there are limited numbers of reports about ZIF-90 membrane fabrication and C4 hydrocarbon separation performance of ZIF-90 membranes.

Herein, we proposed a new method to fabricate thin ZIF-90 membranes (thickness $\sim 3 - 5$ μm) for C4 hydrocarbon separation via Microwave (MW) assisted seeding of ZIF-8 on alumina supports, solvent-assisted linker exchange, and tertiary growth. Even though the cracks formed after drying, saturated drying technique was applied to reduce the formation of cracks efficiently. In addition, several binary gas permeation measurements have been conducted to obtain the performance of the as-synthesized ZIF-90 membranes. The gas permeation measurement for our targeted C4 hydrocarbons is still waiting until the equipment and C4 hydrocarbon were ready for permeation measurement.

ACKNOWLEDGMENTS

I wish to thank the members of my dissertation committee: Dr. Hongcai (Joe) Zhou and Dr. Mustafa Akbulut for generously offering their time, support, guidance, and goodwill throughout the preparation and review of this thesis.

I would also like to thank my thesis advisor Dr. Hae-Kwon Jeong. The door to Dr. Jeong's office was always open whenever I have issues or had a question about my research or writing. He consistently steered me in the right the direction whenever he thought I needed it.

I would also like to thank my colleagues, Moonjoo Lee, who gave me a lot of support and guidance in my research. It is a great pleasure to work with her in my master's career. Besides, thanks to Mohamad Rezi Abdul Hamid's patience to help me whenever I have a problem with my research and coursework, I can complete my project. Most importantly, I would like to thank Febrian Hillman, Jinze Sun, Sungwan Park, Stephanie Bates, Kie Yong Cho ,and Chen Yu, for their help and encouragement.

Finally, I must express my very profound gratitude to my parents and friends for providing me with unfailing supports and continuous encouragement throughout my years of study and through the process of researching and writing this thesis. This accomplishment would not have been possible without them. Thank you.

CONTRIBUTORS AND FUNDING SOURCES

Contributors

Part 1, faculty committee recognition

This work was supervised by a thesis (or) dissertation committee consisting of Professor Hae-Kwon Jeong and Professor Hongcai Zhou of the Department of Chemistry and Professor Mustafa Akbulut of the Department of Chemical Engineering.

Part 2, student/collaborator contributions

All work for the thesis was completed independently by the student and Dr. Moonjoo Lee.

Funding Sources

This work was made possible in part by National Science Foundation (CBET-1510530) and NPRP under Grant Number 8-001-2-001 from Qatar National Research Fund (a member of Qatar Foundation).

NOMENCLATURE

MOFs	Metal-organic Frameworks
ZIFs	Zeolitic-imidazolate Frameworks
MW	Microwave
CMS	Carbon Molecular Sieve
SALE	Solvent-assisted Linker Exchange
XRD	X-ray Diffraction
SEM	Scanning Electron Microscopy
FTIR	Fourier Transform Infrared
ICA	Imidazolate-2-carboxaldehyde
mIm	2-Methylimidazole
MMMs	Mix-matrix Membranes
SOD	Sodalite
LPG	Liquefied Petroleum Gas

TABLE OF CONTENTS

	Page
ABSTRACT.....	ii
ACKNOWLEDGMENTS	iii
CONTRIBUTORS AND FUNDING SOURCES	iv
NOMENCLATURE	v
TABLE OF CONTENTS.....	vi
LIST OF FIGURES	viii
LIST OF TABLES.....	xi
CHAPTER I INTRODUCTION.....	1
CHAPTER II BACKGROUND AND LITERATURE REVIEW.....	3
2.1 C4 hydrocarbon industry	3
2.2 Separation technologies development for hydrocarbon separation	6
2.3 Gas transport through membranes	10
2.4 Zeolitic-imidazolate framework (ZIF) membranes	14
2.4.1 Introduction of ZIFs	14
2.4.2 Fabrication of ZIF membranes	14
2.4.3 Challenges	19
CHAPTER III CHARACTERIZATION AND EXPERIMENTS.....	22
3.1 Materials	22
3.2 Characterization	22
3.2.1 Powder X-ray Diffraction (PXRD)	22
3.2.2 Scanning Electron Microscopy (SEM)	23
3.2.3 Fourier Transform Infrared (FTIR) Spectroscopy	23
3.3 Experiments	24
3.3.1. α -alumina supports	24
3.3.2. ZIF-8 seeded supports	24
3.3.3. ZIF-90 and ZIF-8-90 seeded supports	25
3.3.4. ICA solvent-assisted linker exchange (SALE) on ZIF-8 seeded supports	26
3.3.5. Secondary growth of ZIF-90 membranes	26
3.3.6. Gas permeation measurement	27

CHAPTER IV ZIF-90 FILMS AND MEMBRANES FABRICATION	28
4.1 <i>In situ</i> method	28
4.2 Secondary growth (seeded) method	29
4.2.1 Heteroepitaxial growth on ZIF-8 seeded supports	30
4.2.2 Secondary growth on ZIF-90 seeded supports	31
4.2.3 Tertiary growth on ICA linker exchanged ZIF-8 seeded supports	39
CHAPTER V ELIMINATION OF CRACKS ON ZIF-90 MEMBRANES	43
5.1 The crack formation	43
5.2 Approaches to reduce crack formation	44
5.2.1 Saturated drying	44
5.2.2 Saturated drying with less volatile solvent (DMF, Ethanol)	44
5.2.3 Others	45
CHAPTER VI CONCLUSION AND FUTURE WORKS.....	47
6.1 Conclusion	47
6.2 Future works	47
6.2.1 Effective way to eliminate the cracks and gas permeation measurements of C4 hydrocarbons for defect-free ZIF-90 membranes	47
6.2.2 Using polymeric hollow fibers as substrates	48
6.2.3 Post-synthetic modifications by linker exchange	49
REFERENCES	50

LIST OF FIGURES

	Page
Figure 1. U.S. butane market revenue by application, 2014-2025, (USD Billion) Copyright 2018, CRAND VIEW RESEARCH.....	3
Figure 2. Industrial applications of C4 hydrocarbons. Polymers and polymer applications are highlighted in orange; fuels and fuel additives are highlighted in green. LPG=liquefied petroleum gas; MTBE=methyl-tert-butyl ether; ETBE=ethyl-tert-butyl ether; BHT=butylated hydroxytoluene; BHA=butylated hydroxyl anisole; SBR=styrene butadiene rubber. Reproduced with permission ² . Copyright 2017, John Wiley & Sons, Inc.	5
Figure 3. Relative energy use for separation technologies ⁶ . Copyright 2005, U.S. Department of Energy, Energy Efficiency and Renewable Energy report "Materials for Separation Technologies: Energy and Emission Reduction Opportunities."	7
Figure 4. Comparison of the separation performance of various membranes on porous tubular supports for n-butane/i-butane separation at 293–373 K. MFI membranes in literatures ⁷⁻¹⁴ (□) [11,26,37–43] and this study, and carbon membranes ⁸ (●) and zeolite membranes from Rongfei Zhou et al. ⁹ (■). The upper bond for carbon membranes (solid green line) and MFI membranes (solid black line) are shown. Reproduced with permission ⁹ . Copyright 2017, Elsevier.	9
Figure 5. The diffusion mechanism for gas separation membranes. Copyright CO2CRC, Australia.	10
Figure 6. Pressure-driven permeation of a one-component solution through a membrane according to solution-diffusion model. Reproduced with permission ¹² . Copyright 1995, Elsevier.....	11
Figure 7. Schematic illustration of the membrane synthesis using the counter-diffusion in situ method. Reproduced with permission ¹⁶ . Copyright 2013, American Chemical Society.	15
Figure 8. (a) The illustration for the rapid microwave-assisted in situ synthesis of mixed linker ZIF-7-8 membranes and (b) comparison of effective pore aperture of ZIF-8, ZIF-7, and mixed linker ZIF-7-8. d_e = effective aperture size. Reproduced with permission ¹⁷ . Copyright 2018, American Chemical Society.	16
Figure 9. Scheme of preparation of ZIF-90 membranes by using 3-aminopropyltriethoxysilane (APTES) as the covalent connection between ZIF-90 film and alumina substrate by	

imine condensation reaction. Reproduced with permission ¹⁸ . Copyright 2010, American Chemical Society.....	17
Figure 10. Schematic illustration of rapid microwave-assisted seeding process (a) the substrates saturated with metal precursor solution in ligand solution (b) the reaction zone at the surface of the substrate under MW (c) the seed crystals formed by heterogeneous nucleation near the surface of the substrate. Reproduced with permission ¹⁹ . Copyright 2013, The Royal Society of Chemistry.....	18
Figure 11. SEM images for (a)(d) in situ growth on a bare alumina substrate (b)(e) modified substrate via MW(1.5 min) in ICA solution (c)(f) amended substrate via solvothermal (60°C, 24hr) process in ICA solution.	29
Figure 12 . ZIF-90 membranes growth on ZIF-8 seeded support (a) top view of membranes and (b) cross-section view.	31
Figure 13. SEM images for ZIF-90 and ZIF-8-90 seeded supports: MW-S-ICA (a)Top view (b) cross-section; MW-S-8-90 (c)Top view (b) cross-section; MW-S-90 (a)Top view (b) cross-section; MW-S-90-DMF (a)Top view (b) cross-section.....	32
Figure 14. XRD patterns for seeded supports prepared via different strategies.	32
Figure 15. SEM images for double seeded supports via MW-S-8-90 (a) (b) and MW-S-90 (c) (d).	34
Figure 16. SEM images for seeded supports (MW-S-8-90, MW-S-90, and MW-S-90-DMF) synthesized by different Zn ²⁺ concentrations (left: original, meddle: double, right: 4 times) in MW seeding.	34
Figure 17. ZIF-90 membranes based on different seeded supports (a) MW-S-ICA (b) MW-S-8-90 (c) MW-S-90 (d) MW-S-90-DMF after secondary growth based on growth solution with sodium formate.....	35
Figure 18. SEM images of ZIF-90 membranes growing (a) without sodium formate at 65°C for 4 h (b) with sodium formate at 65°C for 4 h (c) with sodium formate (2 times concentrated) at 65°C for 4 h (d) with sodium formate (4 times concentrated) at 65°C for 4 h. More defects and weird morphology can be observed after secondary growth with the existence of sodium formate in growth solution.....	36
Figure 19. The seeded supports after ICA linker exchange reaction at different reaction time (12, 24,48hr) and concentration of ICA (26mM, 130mM, 390mM).	36
Figure 20. SEM images for ZIF-90 membranes which are synthesized based on seeded supports with ICA linker exchange at different reaction time (12hr, 24hr, 48hr) and concentration of ICA (26mM, 130mM, 390mM).	37

Figure 21. The XRD patterns for ZIF-8 seeded supports and seeded supports after ICA linker exchange reaction with a different time (12h, 24h, 48h), and various ICA concentration (26mM, 130mM, 390mM).	38
Figure 22. Secondary growth with different growth time. 1hr:(a)(b) 2hr:(c)(d) 4hr(e)(f) 12hr(g)(h). The ZIF-90 membranes after 4 hr secondary growth show less roughness and well-intergrown.	39
Figure 23. The ZIF-90 membranes under the same synthesis condition (65°C, 4hr) and seeded supports. (a) poor-intergrown ZIF-90 membranes. (b) well-intergrown ZIF-90 membranes.	40
Figure 24. Schematic illustration of the synthesis of ZIF-90 membranes (a) MW-assisted seeding to form ZIF-8 seeds on the porous support (b) ZIF-8 seeded support (c) ZIF-8-90 seeded support after SALE (d) ZIF-90 membrane with thickness ~ 3 - 5 μm	41
Figure 25. The seeded supports after SALE treatment: (a) Top view, (b) Cross section; ZIF-90 membranes after Tertiary growth: (c) Top view, (d) Cross section.	42
Figure 26. XRD pattern (a)ZIF-90 simulated (b)ZIF-8 seeded support (c)ZIF-8 seeded supports after SALE (d)ZIF-90 membrane synthesized via secondary growth (e)ZIF-90 membrane synthesized via tertiary growth (★) Al_2O_3 supports.....	42
Figure 27. The ZIF-90 membranes after saturated drying with DMF : (a)(b)top view(c)cross-section view; Ethanol: (d)(e)top view(f)cross-section view; Methanol: (g)(h)top view(i)cross-section view.....	45
Figure 28. Permeance as a function of the size of gas molecular.	48

LIST OF TABLES

	Page
Table 1. The physical properties of C4 hydrocarbons. Reproduced with permission. ² Copyright 2017, John Wiley & Sons, Inc.	5

CHAPTER I

INTRODUCTION

C4 hydrocarbon (butane, isobutane, 1-butene, 2-butene, isobutene, and 1,3-butadiene) separation is a significant due to its market size and versatility of these C4 chemicals. For example, butane, flammable and colorless gas, is enormously demanded in the industry. Butane can be extracted from natural gas or obtained during petroleum refining. In refinery process, an appreciable amount of butane can be derived from the stream of gas in cracking units, and butane can be separated from the gas mixture through adsorption, distillation technologies. Isobutane, branched isomers of butane, can be converted from butane via isomerization. The separation process is needed to separate butane and isobutene mixtures from the product of reactor.

Separation of the gas mixture is one of challenging tasks in industry, especially the separation of hydrocarbons in the petrochemical industry. The separation of hydrocarbons such as butane/isobutane mixture was implemented by multiple and relative energy-intensive distillation columns. With the concern about sustainable development and increasing price of energy resources, Membrane-based separation technologies were introduced to separate the targeted gas mixture in industry.

The current membrane market for gas separation is dominated by polymeric membrane mostly because of low production cost, mechanical flexibility. However, polymeric membranes have poor gas separation properties especially for hydrocarbon separation and low chemical/thermal stability. ZIF membranes with high thermal/chemical stability and well-defined pores could be alternatives to surpass the polymeric membranes and replace the conventional energy-intensive gas separation process. ZIF-8 is one of ZIF membranes used for separate the

propylene ($\sim 4.0 \text{ \AA}$)/propane ($\sim 4.3 \text{ \AA}$) due to its effective aperture size $\sim 4.0 \text{ \AA}$ ¹. Because of its impressive propylene/propane separation performance, ZIF-8 garnered much attention in the recent decade. Recently, ZIF-90 emerged as another candidate for C4 hydrocarbon separation because the effective aperture size of ZIF-90 was reported as $\sim 5.0 \text{ \AA}$ which fall in between the size of butane and isobutane. However, all of the previous studies about ZIF-90 membranes do not focus on the separation of C4 hydrocarbon.

In this thesis, we performed the synthesis of thin polycrystalline ZIF-90 membranes on porous α -alumina substrates. Microwave seeding techniques were applied to coat layers of ZIF-8 seed crystals on the surface of substrates. After that, the ICA (ZIF-90 linker) linker exchange was employed to ZIF-8 seeded substrates to produce ZIF-8-90 mix-linker seed crystals. Based on seeded substrates, well-intergrown polycrystalline ZIF-90 membranes with thickness $\sim 3 - 5 \text{ \mu m}$ could be synthesized after tertiary growth. Besides, several strategies were used to eliminate the crack formation of ZIF-90 membranes after drying. Gas permeation measurements for H₂, CO₂, N₂, CH₄, C₃H₆, and C₃H₈ have been collected. Permeation measurement of C4 hydrocarbons such as butane and isobutane will be obtained in the future.

The thesis is composed of several chapters. The following chapter II provides general background and reviews on (1) C4 hydrocarbon and separation in the industry (2) gas transport through microporous membranes and (3) membrane-based technology for hydrocarbon separation. Chapter III indicates the experiment material, experiments, and characterization tool. The research results and detailed discussions are presented in Chapter IV. The crack formation on ZIF-90 membranes was discussed in Chapter V. Lastly the conclusion, and future works are provided in the final chapter.

CHAPTER II

BACKGROUND AND LITERATURE REVIEW

2.1 C4 hydrocarbon industry

C4 hydrocarbon (butane, 1-butene, 2-butene, isobutene, 1,3-butadiene, and isobutane) are significant research topic because of their importance in industry. Butane is colorless and flammable gas. Isobutane is butane's isomer. Butane is one of the major components in liquefied petroleum gas (LPG), and it is liquefiable at a moderate pressure at a temperature near the freezing point. That is why it is suitable for transportation and storage in the form of liquid. The typical applications of butane including a cigarette lighter, aerosol propellant, calibration gas, refrigerant, fuel additive and chemical feedstock in the petrochemical industry. The market size of butane was estimated at USD 60.01 billion in 2015. Moreover, significant growth of demand and gradually rise of revenue in the market is expected.

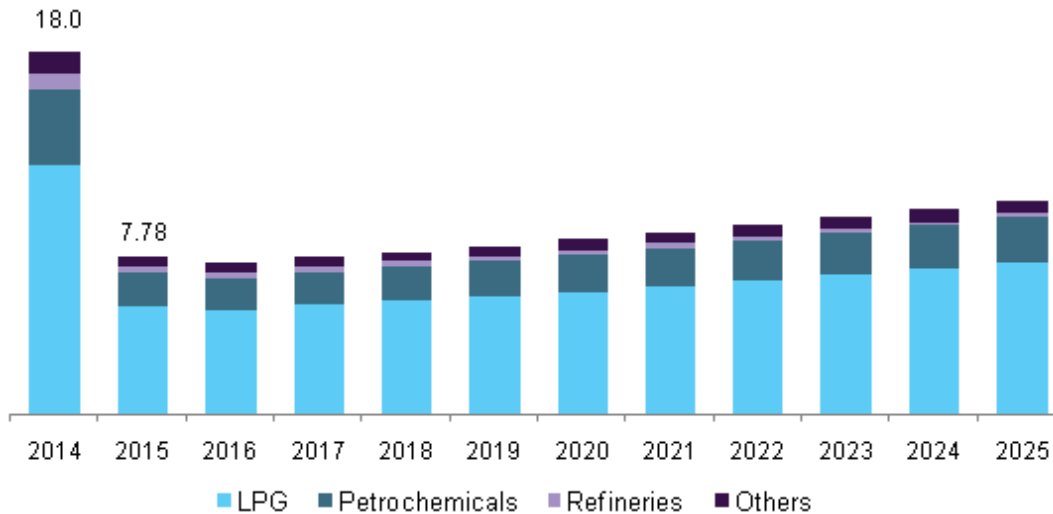


Figure 1. U.S. butane market revenue by application, 2014-2025, (USD Billion) Copyright 2018, CRAND VIEW RESEARCH. Reprinted with permission.

Butane can be extracted from natural gas or gas stream from cracking units in petroleum refining process. Normal butane can be simply converted into isobutane through isomerization. The isomerization of normal butane occurs in a reactor under 15 atm at 300°C. The product from the isomerization reactor contains the mixture of isobutane and unreacted normal butane. Therefore, the separation process is required to obtain a high purity of butane and isobutane. Isomerization of normal butane to produce isobutane is crucial since it can provide feedstock for alkylation in the oil industry.

1,3-Butadiene is another important C4 hydrocarbons. It is usually utilized for the manufacture of synthetic rubbers and elastomers. Furthermore, global 1,3-butadiene market is projected to achieve a valuation of \$ 33.5 billion in 2017-2024 according to the reports from Research Nester. It can be obtained from the steam cracking process of ethylene and olefin production. Gaseous isobutene is also crucial C4 hydrocarbons in the petrochemical building block. As large as 15 million tons of isobutene every year are derived from oil and applied to the production of plastic and elastomers. N-butenes have a large impact in the industry owing to the large demand for alkylate gasoline, detergent alcohols, synthetic lubricants, and plasticizers.

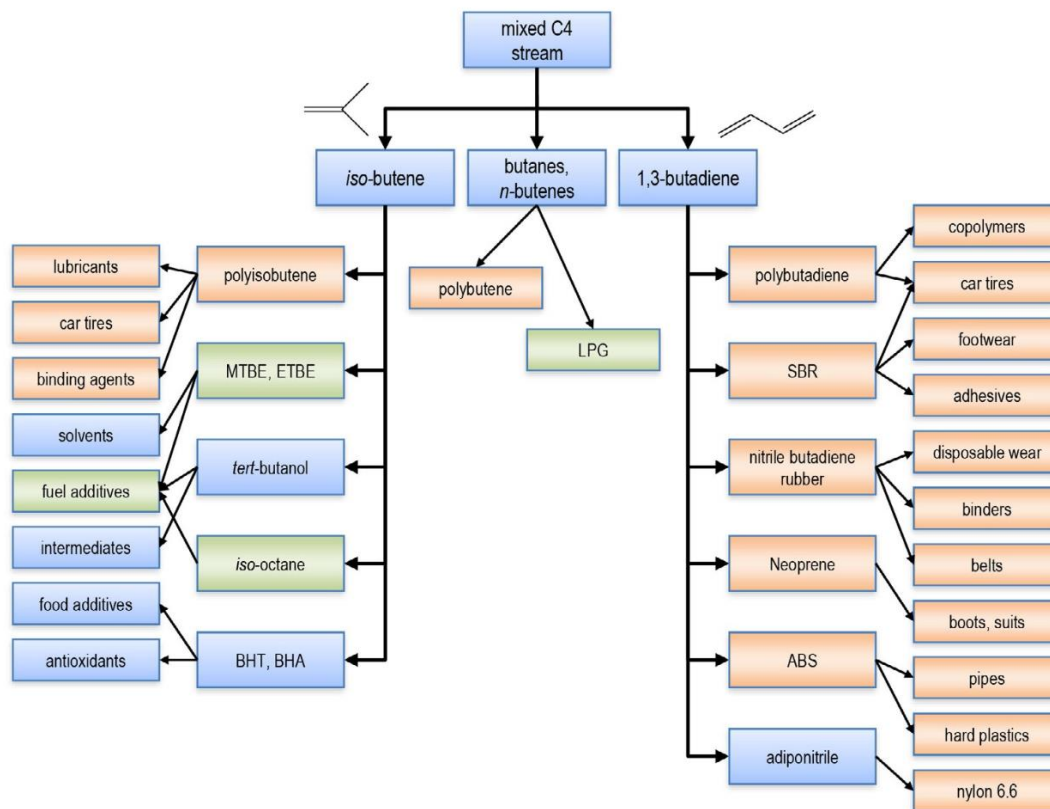


Figure 2. Industrial applications of C4 hydrocarbons. Polymers and polymer applications are highlighted in orange; fuels and fuel additives are highlighted in green. LPG=liquefied petroleum gas; MTBE=methyl-tert-butyl ether; ETBE=ethyl-tert-butyl ether; BHT=butylated hydroxytoluene; BHA=butylated hydroxyl anisole; SBR=styrene butadiene rubber. Reproduced with permission². Copyright 2017, John Wiley & Sons, Inc.

Table 1. The physical properties of C4 hydrocarbons. Reproduced with permission.² Copyright 2017, John Wiley & Sons, Inc.

Compound	B.p.[k]	Kinetic diameter[Å]	Polarizability[10^{-25} cm^3]	Dipole moment ^[a] [$\times 10^{18} \text{ esucm}$]
butane	272.66	4.687	82	0.05
isobutane	261.34	5.278	81.4-82.9	0.132
1-butene	266.92	4.460	81	0.359-0.438
cis-2-butene	276.87	4.940	82	0.30
trans-2-butene	274.03	4.310	81.82	0.00
1,3-butadiene	268.62	4.310	86.4	0.00
isobutene	266.25	4.840	80	0.50

[a] 1 Debye = 10^{-18} esu cm.

2.2 Separation technologies development for hydrocarbon separation

Since those C4 hydrocarbons need to have a certain degree of purities for further applications, especially for polymerization, the separation processes are essential. Unfortunately, separation of these components is exceptionally costly and challenging due to similar physical properties of C4 hydrocarbons (Table 1). For example, isobutane is separated from n-butane by distillation which is thermal driven and energy-intensive process. Besides, 1,3-Butadiene is often separated from mixtures by extractive distillation, and distillation process is considered as energy intensive separation process. Therefore, some alternative separation technologies are introduced to replace the conventional thermal driven separation process to save energy and expenditure.

Adsorption by using microporous materials such as zeolites and MOFs is promising alternatives to offer energy-efficient separation. The adsorption process is applied widely by gas and liquid purification and segregation in the chemical, petrochemical industry. Adsorption process can sufficiently separate the mixture of components based on the different affinity of elements to adsorbents. The adsorbents are then regenerated through desorption of gases or molecules. It is competitive since high purity product with a minute concentration of contaminant and large production rate can be achieved. Nevertheless, the applications are confined to hundred per million of the concentration of components to be removed. Moreover, once saturation is reached, the adsorbents need to be regenerated.

Membrane-based separation is another promising alternative among non-thermal driven processes to replace conventional energy-intensive process due to several advantages. First of all, it is energy efficient (as shown in Figure 3) because no phase change involved. Second, it is simple regarding operation and convenient for small-scale separation. Lastly, since adsorbents are not essential, membranes based technology is cost effective³⁻⁵. Consequently, membrane-

based separation technologies including high-performance polymers, carbon molecular sieve (CMS), zeolite, and MOFs membranes are developed to address the issues in hydrocarbon separation.

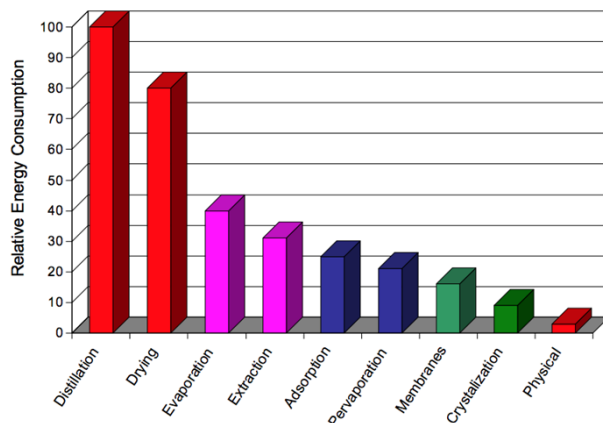


Figure 3. Relative energy use for separation technologies⁶. Figure taken from USDOE, Office of Energy Efficiency and Renewable Energy, Advanced Manufacturing Office (formerly the Industrial Technologies Program) report titled “Materials for Separation Technologies: Energies and Emission Reduction Opportunities” (2015), and reproduce with permission from BCS, LLC”.

Polymers are widely accepted material as membranes for gas separation because it is processable and easy-to-get. Numerous of studies on polymeric membranes have been conducted, but we can hardly find the one can be suitable for hydrocarbon separation because of low permeability or selectivity. Even though polyimide-based membranes display enhanced selectivity for olefins, the selectivity reduces dramatically in gas mixture owing to the intensive plasticization effect. In order to improve the separation properties of polymeric membranes, some criteria are suggested. (1) Sizeable free volume with inflexible, rigid polymer structures. (2) Long-term stability and durability under practical operating conditions. In fact, however, these can be achieved by inorganic materials such as zeolites, carbon molecular sieve, and ZIFs which have garnered extensive attention lately.

Carbon molecular sieves (CMS) membranes can offer excellent performance in separation of gas mixtures such as hydrocarbons. Moreover, a carbon membrane can be tuned by pore size to bring about impressive separation performance for a given combination of gases as a result. But, commercial applications are still rarely found. Large-scale production is quite challenging owing to high temperature required during the production, the breaking of the fiber during mounting, and the fragility of carbon fibers and stability over time. Also, the CMS fibers are vulnerable to oxidizing agents, water vapors, contaminants which would block the pores⁷. It is still a long road to prepare the high-quality CMS membranes which were widely accepted in the industry of separation.

Both zeolites and ZIFs have well-defined pore structure and excellent thermal and chemical stability in comparison with other membrane materials. However, ZIFs is more competitive than zeolites because the accessibility of chemical modification of the organic linkers in the frameworks can tune the properties of materials for specific applications. Moreover, the “gate-opening” effect induced by flopping motion of linkers and host-guest interactions brings about flexible frameworks and potential demand for separating a wide range of gas mixtures³.

Pseudo-Robeson plots have been created for reliable estimation of the permeance and selectivity that can be anticipated for the best membrane materials. Figure 4 shows the Pseudo-Robeson plots for butane isomers separation performance. According to the scheme for n-butane/i-butane separation, MFI type zeolites showed promising performance for butane/i-butane separation. MFI zeolite (silicalite-1 and ZSM-5) has elliptical channels along the axis with window size of $5.1 \times 5.5 \text{ \AA}$ and $5.6 \times 5.3 \text{ \AA}$ -sized elliptical channels running along the b axis.

Therefore, MFI zeolites are suitable for separating those C4 hydrocarbons with size around 4.3 Å ~ 5.2 Å.

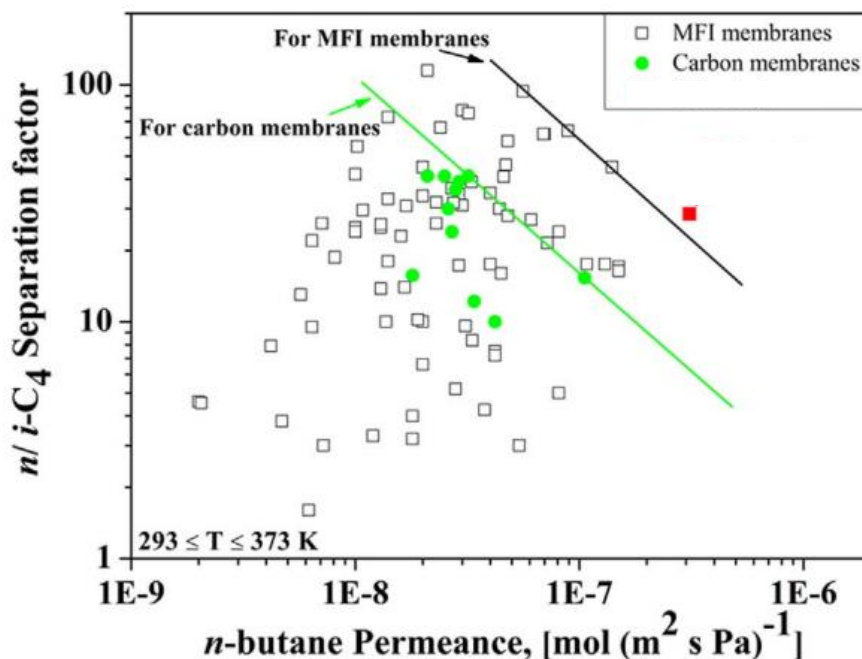


Figure 4. Comparison of the separation performance of various membranes on porous tubular supports for n-butane/i-butane separation at 293–373 K. MFI membranes in literatures^{7–14}(□) [11,26,37–43] and this study, and carbon membranes⁸(●) and zeolite membranes from Rongfei Zhou et al.⁹(■). The upper bond for carbon membranes (solid green line) and MFI membranes (solid black line) are shown. Reproduced with permission⁹. Copyright 2017, Elsevier.

Recently, Nair and his coworkers indicated that ZIF-90, consisting of zinc ion and imidazolate-2-carboxaldehyde, has effective aperture size ~ 5.0 Å¹⁰. ZIF-90 with 5.0 Å aperture size is suitable for C4 hydrocarbon separation since the kinetic size of C4 hydrocarbon are in the range of 4.3 Å ~ 5.2 Å, especially for n-butane (~ 4.687 Å) /isobutene (~ 5.278 Å). According to their diffusivity study of ZIF-90 powder, the diffusive selectivity of butane isomers can be up to 700, which is almost 7 times larger than current zeolite membranes could achieve. Furthermore, ZIF-90 has an advantage over other ZIFs because modifiable functional groups (aldehyde groups, C=O) in the frameworks offer the possibility to tailor the separation properties via ligand

covalent functionalization. However, to the author's best knowledge, very few publications are available in literature related to ZIF-90 membranes for C4 hydrocarbons separations.

In an attempt to synthesize ZIF-90 membranes for gas separation, reviews of ZIF membranes fabrication and challenges to produce high-quality membranes are discussed in section 2.4.

2.3 Gas transport through membranes

Selectivity and permeance are both essential properties of membranes in the gas separation process. To understand the mechanism of gas separation through membranes can help design membranes with satisfied performance as a result.

The common mechanisms for gas separation in membranes can be classified as Knudsen diffusion, molecular sieving, solution diffusion and surface diffusion. Knudsen diffusion is correlated to the mean free path of the molecules involving. Molecular sieving is the mechanism by which the gases are separated based on the size of molecular (kinetic diameter). Solution-diffusion and surface diffusion are, on the other hand, concerned with the affinity between molecules and membranes¹¹.

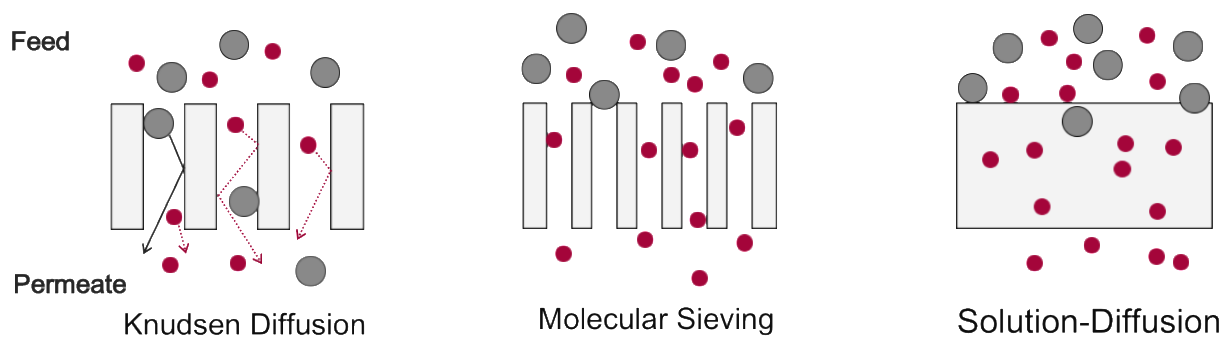


Figure 5. The diffusion mechanism for gas separation membranes.

In case of polymeric membranes, inorganic membranes (zeolites, MOFs), and MMMs, solution-diffusion model¹² can be employed to describe the phenomenon of gas transport through membranes.

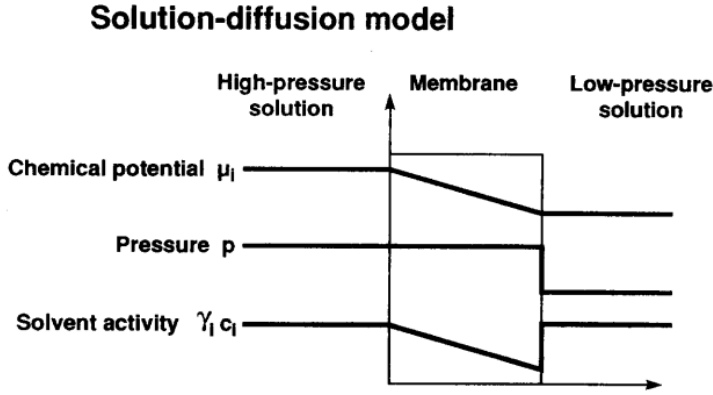


Figure 6. Pressure-driven permeation of a one-component solution through a membrane according to solution-diffusion model. Reproduced with permission¹². Copyright 1995, Elsevier.

In solution-diffusion model, the pressure throughout the membrane is assumed to be equal to the pressure at feed side, and smooth chemical potential gradient exists across the membrane. The flux of component i can be described as:

$$J_i = -L_i \frac{d\mu_i}{dx} \quad (1)$$

($\frac{d\mu_i}{dx}$ is the gradient in chemical potential of component i , and L_i is the coefficient of proportionality)

Plus, the driving force induced by concentration and pressure can be expressed as:

$$d\mu_i = RT d\ln(\gamma_i c_i) + v_i dP \quad (2)$$

(c_i is molar concentration of component i , γ_i is the activity coefficient, v_i is molar the volume of component i , and P is pressure)

Since the pressure difference is negligible within the membrane, combining Equation(1) and Equation(2):

$$J_i = -\frac{RTL_i}{c_i} \cdot \frac{dc_i}{dx} \quad (3)$$

According to Fick's law:

$$J_i = -D_i \frac{dc_i}{dx}$$

where $\frac{RTL_i}{c_i}$ can be replaced by D_i (diffusion coefficient)

Given the integration through the thickness of membrane:

$$J_i = \frac{D_i(c_{i0} - c_{il})}{l} \quad (4)$$

For gas separation membrane, the pressure P_0 is given at feed side of the membrane. On the other side, gas is removed a lower pressure P_l at the permeate side of the membrane. To start with, the chemical potential is equal in thorough system of both sides of the membrane. For gas phase (compressible), the chemical potential is given by:

$$\mu_i = \mu_i^0 + RT \ln(\gamma_{i0} c_{i0}) + RT \ln\left(\frac{P}{P_{isat}}\right) \quad (5)$$

where P_{isat} is saturation vapor pressure of i

For the membrane (m) which is incompressible,

$$\mu_i = \mu_i^0 + RT \ln(\gamma_{i0(m)} c_{i0(m)}) + v_i(P - P_{isat}) \quad (6)$$

By equating the chemical potentials at the feed side interface of the membrane:

$$\mu_i^0 = \mu_i^0(\text{membrane})$$

$$\mu_i^0 + RT \ln(\gamma_{i0} c_{i0}) + RT \ln\left(\frac{P_0}{P_{isat}}\right) = \mu_i^0 + RT \ln(\gamma_{i0(m)} c_{i0(m)}) + v_i(P - P_{isat}) \quad (7)$$

By rearrangement,

$$c_{i0(m)} = \gamma_i / \gamma_{i0(m)} \cdot P_0 / P_{isat} \cdot c_{i0} \cdot \exp(-v_i \cdot (P_0 - P_{isat}) / RT) \quad (8)$$

The exponential term should be close to one,

$$c_{i0(m)} = \gamma_i / \gamma_{i0(m)} \cdot P_0 / P_{isat} \cdot c_{i0} \quad \text{where } c_{i0} \cdot P_0 \text{ is partial pressure of } i \text{ (} P_{i0} \text{)} \quad (9)$$

$$c_{i0(m)} = \gamma_i / \gamma_{i0(m)} \cdot P_{i0} / P_{isat} \quad \text{where } \gamma_i / \gamma_{i0(m)} \cdot 1 / P_{isat} \text{ is sorption coefficient (} K_i^G \text{)} \quad (10)$$

$$c_{i0(m)} = K_i^G \cdot P_{i0} \quad (11)$$

By doing the same way to the permeate side interface of the membrane:

$$c_{il(m)} = K_i^G \cdot P_{il} \quad (12)$$

Applying those to Equation (4),

$$J_i = D_i K_i^G (P_{i0} - P_{il}) / l \quad \text{where } D_i K_i^G \text{ is permeability coefficient (} P_i^G \text{)} \quad (13)$$

$$J_i = P_i^G (P_{i0} - P_{il}) / l \quad (14)$$

It is widely used to predict or describe the properties of the membranes for gas separation.

2.4 Zeolitic-imidazolate framework (ZIF) membranes

2.4.1 Introduction of ZIFs

Zeolitic-imidazolate frameworks (ZIFs) are large sub-family of Metal-organic frameworks (MOFs). They topologically resemble the zeolites but are comprised of transition metal (usually Zinc and Cobalt) ions and imidazole-based ligands. Because of a variety of linkers are available, over 150 kinds of ZIFs materials have been discovered so far. With permanent porosity (window size $< 7 \text{ \AA}$), they are suitable for molecular sieving-based membrane gas separation. Moreover, the flexibility of the frameworks leads to high permeability and satisfied selectivity at the same time. Furthermore, ZIFs are believed to have excellent thermal and chemical stability. Consequently, ZIFs have attracted a lot of attention, and many applications are found, especially the unprecedented opportunities in gas separation and storage technology. In the field of gas separation membranes research, plenty of ZIFs (ZIF-7, ZIF-8, ZIF-22, ZIF-69, ZIF-78, ZIF-90, ZIF-93, ZIF-95, ZIF-100, and ZIF-67) have been employed to synthesize supported ZIF membranes. Depending on different properties of those ZIF materials, a wide range of applications can be expected, including Hydrogen separation (e.g., H_2/N_2 , H_2/CO_2 , H_2/CH_4 , $\text{H}_2/\text{C}_2\text{H}_6$, $\text{H}_2/\text{C}_3\text{H}_8$), natural gas/biogas purification (CO_2/CH_4), and olefin/paraffin separation (e.g., propylene/propane, ethylene/ethane). However, the ZIF membranes synthesis and its scalability remain the most significant barrier to commercialize those membranes in the market.

2.4.2 Fabrication of ZIF membranes

2.4.2.1 *In situ* methods

In situ method means the one-step synthesis of membranes based on modified or unmodified supports. There are several kinds of ZIF membranes synthesized by this technique.

Caro et al. reported well-intergrown ZIF-8 membranes grew on unmodified titania substrates with in situ MW-assisted solvothermal approach¹³. ZIF-69 membranes can be manufactured based on unmodified alumina substrates via *in situ* solvothermal approach¹⁴. However, directly synthesis is quite challenging because of unfavorable heterogeneous nucleation on the bare alumina supports. Moreover, the ZIF membrane and its substrate interact poorly and that cause instability in the practical applications for gas separation. Jeong et. al.¹⁵ came up with the thermal modification applied to alumina substrates and synthesize ZIF-8 films based on these modified supports. Counter-diffusion method (Figure 7) which was reported by Kwon and Jeong¹⁶ is another alternative *in situ* solvothermal approaches to growing well-intergrown ZIF-8 membranes with improved microstructure. The porous alumina substrates were soaked in metal precursor solution until saturated with metal ions firstly and then treated with ligand solution in Teflon autoclave for hours at 120°C. Counter diffusion of ions and ligands occurred at the interface of solution and surface of the substrate. The interface provided the reaction zone to grow crystals from the substrate surface. As a result, the membranes synthesized through this approach show remarkable mechanical stability with thickness $\sim 1.5\mu\text{m}$.

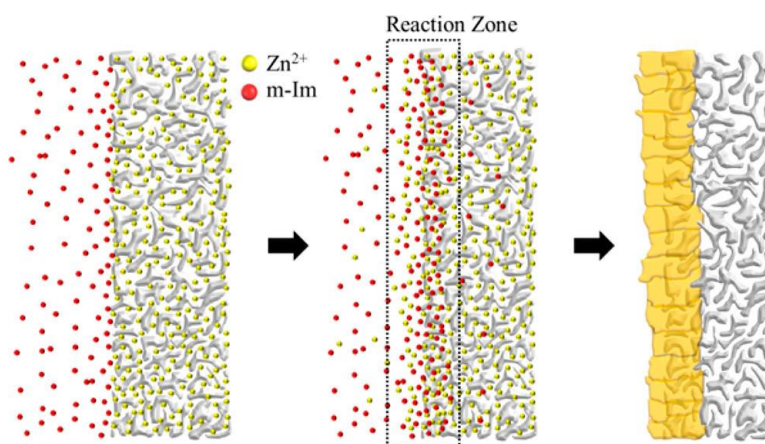


Figure 7. Schematic illustration of the membrane synthesis using the counter-diffusion in situ method. Reproduced with permission¹⁶. Copyright 2013, American Chemical Society.

In situ synthesis of mixed-linker composite ZIF membranes were successfully synthesized under MW irradiation by Febrian Hillman and his coworkers¹⁷. Briefly, the alumina substrates were placed into metal solution to be saturated with zinc ion. After that, the alumina substrates were soaked in a reactor containing a mixed-linker solution (ZIF-7 and ZIF-8 linkers) and shine MW for ~90 seconds. Well-intergrown polycrystalline ZIF-7-8 membranes with thickness ~ 1 μm can be obtained within extremely short time. The scheme of synthesis procedure is shown in Figure 8. They also claim that the effective aperture size can be tuned by direct mixed-linker synthesis.

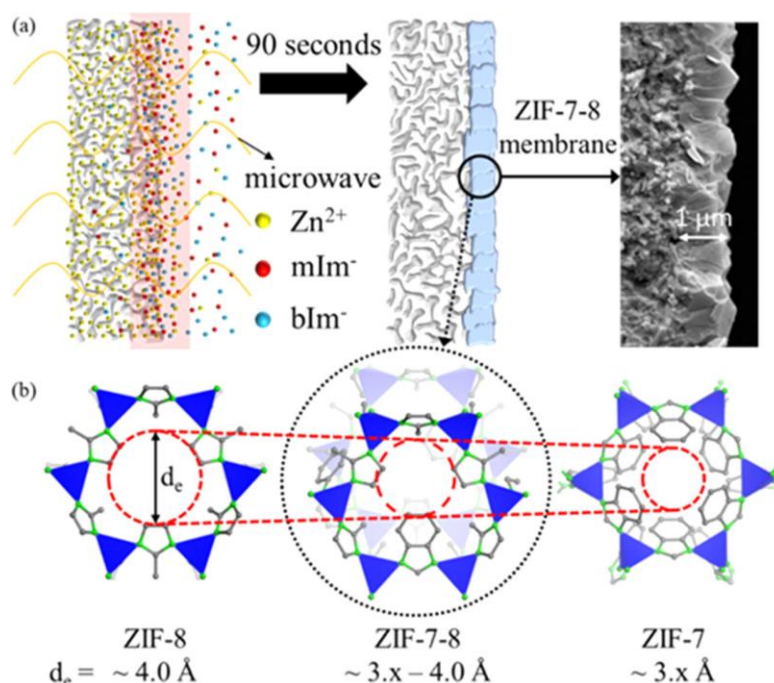


Figure 8. (a) The illustration for the rapid microwave-assisted in situ synthesis of mixed linker ZIF-7-8 membranes and (b) comparison of effective pore aperture of ZIF-8, ZIF-7, and mixed linker ZIF-7-8. d_e = effective aperture size. Reproduced with permission¹⁷. Copyright 2018, American Chemical Society.

ZIF-90 can be synthesized based on modified alumina supports as reported from Caro et. al.¹⁸. To begin with, the hydroxyl groups from alumina support react with ethoxy groups from 3-

aminopropyltriethoxysilane (APTES). Next, the amino groups and aldehyde groups in ZIF-90 linkers would react via imines condensation to provide a robust covalent connection between ZIF-90 membranes and modified alumina substrates (Figure 9). As a result, they can produce a continuous polycrystalline ZIF-90 membrane with $\sim 20\mu\text{m}$ thickness and high hydrogen permselectivity.

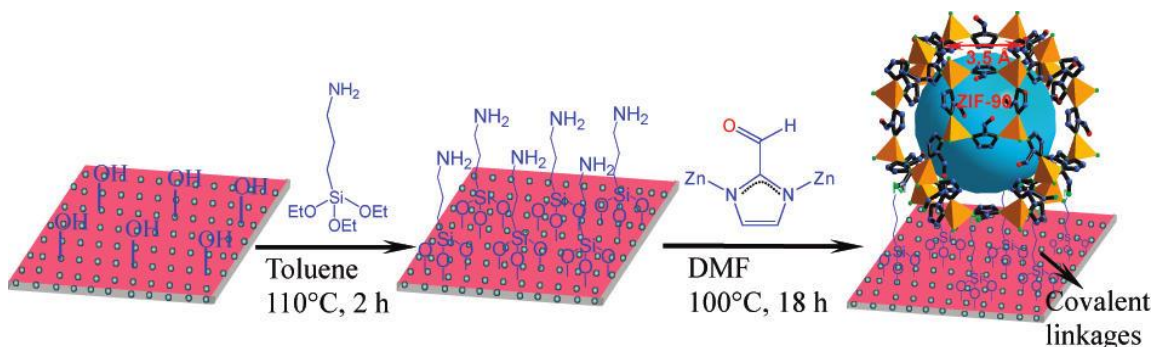


Figure 9. Scheme of preparation of ZIF-90 membranes by using 3-aminopropyltriethoxysilane (APTES) as the covalent connection between ZIF-90 film and alumina substrate by imine condensation reaction. Reproduced with permission¹⁸. Copyright 2010, American Chemical Society.

2.4.2.2 Secondary growth (seeded) methods

In addition to in situ method, seeding method along with secondary growth offers a way to prepare ZIF membranes. Seeding involves coating single or several layers of seed crystals on the surface of substrates and secondary growth applied by the solvothermal approach. Secondary growth with seeding technique brings about better microstructure and strong interaction between substrates and ZIF membranes. Some seeding methods have been developed including dip coating, slip coating, manual rubbing, and MW-assisted seeding. MW-assisted seeding method reported by Kwon and Jeong¹⁹ (Figure 10) was employed to synthesize ZIF-8 membranes. MW-assisted seeding could offer densely-packed and strongly-attached seed crystals on the porous supports rapidly, and well-intergrown ZIF-8 membranes were obtained after secondary growth.

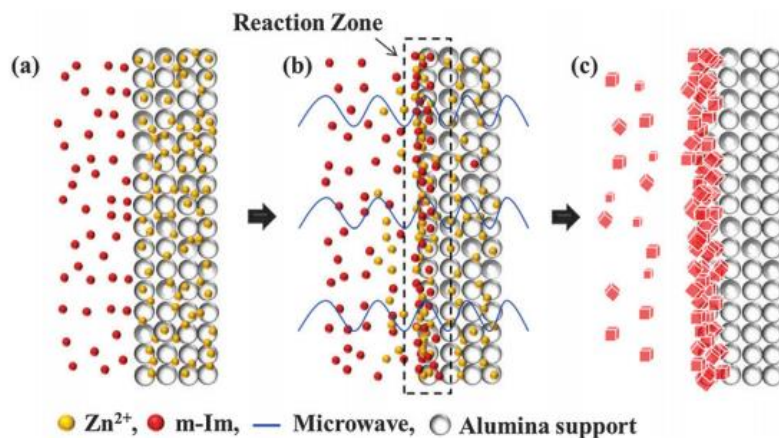


Figure 10. Schematic illustration of rapid microwave-assisted seeding process (a) the substrates saturated with metal precursor solution in ligand solution (b) the reaction zone at the surface of the substrate under MW (c) the seed crystals formed by heterogeneous nucleation near the surface of the substrate. Reproduced with permission¹⁹. Copyright 2013, The Royal Society of Chemistry.

Dong et al. propose reactive seeding method and secondary growth to prepare ZIF-78 membranes on ZnO substrates. The seeding process was conducted by in situ crystal growth. After secondary growth, the crack-free ZIF-78 membranes with thickness $\sim 25\mu\text{m}$ can be obtained. Furthermore, ZIF-78 membranes demonstrate the satisfied performance of H₂/CO₂ separation.

Brown et. al.²⁰ applied dip-coating method on polymeric hollow fibers and secondary growth to synthesize thin ZIF-90 membranes on polymeric hollow fibers. This work opens up the way to prepare hollow-fiber-based ZIF membranes that are believed to be able to scale up for the production of large-surface-area membrane modules.

2.4.3 Challenges

2.4.3.1 Weak substrate bonding

Weak bonding between membrane and substrate is a common challenge facing while preparing ZIF membranes. Therefore, chemical modification on the substrate is an effective strategy to improve heterogeneous nucleation and in situ growth of membranes. For instance, a covalent functionalization was employed to prepare ZIF-90 membranes using APTES to modify the -OH bond on the alumina substrates and provide covalent bonding between ZIF-90 membranes and substrates¹⁸. Some ZIF membranes can be synthesized via direct synthesis methods. Nevertheless, it is often difficult to control the crystallization on the substrate since the crystallization would be affected by many factors. In an attempt to enhance the availability of high-quality membranes, seeding along with secondary growth was developed.

2.4.3.2 Crack formation during fabrication

Crack formation is a vital issue in the manufacture of ZIF membranes and will lead to reduced performance of membranes for gas separation. ZIFs are polycrystalline materials, thus, mechanically brittle. Accordingly, the approach to prevent cracks is a subject of importance.

So far, the cracks on the ZIF membranes could result from (1) thermal stress during the cooling after synthesis at elevated temperature and (2) drying of membranes after washing²¹. Rapid cooling after synthesis could likely give rise to cracks induced by a mismatch in thermal expansion in membranes and substrates. ZIF-69¹⁴ has been reported to need slow cooling after synthesis. Natural cooling for a long time could alleviate the issue of crack formation resulting from rapid cooling.

Drying of ZIF membranes could also cause crack formation. For ZIF membranes, crack formation could be ascribed to the asymmetric stress induced by capillary force or drying stress

caused by different shrinkage rate between the surface and inside of the membranes. By using a surfactant to decrease capillary stress, the effect of capillary force can sufficiently reduce and reduce the formation of cracks^{22,23}. For the cracks induced by drying stress, decreasing drying rate via saturated drying (drying at nearly saturated condition) could be a useful strategy to eliminate the crack formation in drying process^{22,24}.

2.4.3.3 Preparation of ultrathin membranes

Tsapatsis²⁵ claimed that the thickness of zeolites membranes requires to being well below ~ 50 nm for specific separation to save the cost of making zeolites membranes and increase the throughput by order-of-magnitude as compared to the current state of the art. The same might be right on ZIF membranes. However, it is formidable task to obtain ZIF membranes with sub-micron thickness because of (1) increasing opportunity for poor grain boundary structure and (2) the surface roughness of supports²⁶. Several sub-micro ZIF-8 membranes were reported ,but none of them showed promising gas separation properties²⁷⁻²⁹. In the recent paper by Kwon et al., thin ZIF-8 membranes with thickness ~ 300 – 400 nm were prepared by merging the ZIF-8 seed crystals in the presence of a ligand vapor at elevated temperature. Even if high propylene/propane separation factor could be achieved, unexpectedly low propylene permeance was obtained at the same time owing to the presence of an excess of linkers in sodalite (SOD) cages which hinder the gas transportation through the pores. These reports mentioned above have demonstrated the difficulties faced to produce thin ZIF membranes with excellent gas separation properties.

2.4.3.4 Others

In spite of promising high-quality gas separation performance of ZIF membranes, there are some obstacles needed to be overcome. It is true that ZIFs are thought of as outstanding membranes for gas separation in lab scale, but its development for practical applications falls into a stagnant, and the scale-up technologies are needed to bring ZIF membranes into the market. Scale-up of ZIF membranes is quite challenging. In the first place, the cost of the porous substrates and organic ligands are expensive. Also, hydrothermal and solvothermal synthesis process isn't efficient in large-scale production. The large area of high-quality membranes required for commercialization is one of the hurdles as well.

CHAPTER III

CHARACTERIZATION AND EXPERIMENTS

3.1 Materials

Alpha- Al_2O_3 powder (CR6, Baikowski) was used to prepare alumina disks, and polyvinyl alcohol (PVA 500, Duksan) was used as a binder for alumina disk preparation. Zinc nitrate hexahydrate ($\text{Zn}(\text{NO}_3)_2 \cdot 6\text{H}_2\text{O}$, 98%, Sigma-Aldrich) and imidazole-2-carboxaldehyde ($\text{C}_4\text{H}_4\text{N}_2\text{O}$, 99.99%, 97%, Alfa Aesar) were used as metal sources. 2-methylimidazole ($\text{C}_4\text{H}_6\text{N}_2$, 99%, Sigma-Aldrich) was used as an organic ligand, and sodium formate (HCO_2Na , 99%, Sigma-Aldrich) was utilized as a deprotonating agent. Methanol (CH_3OH , > 99%, Alfa Aesar), deionized water, N,N-Dimethylformamide ($\text{HCON}(\text{CH}_3)_2$, ACS, >99.8%, Alfa Aesar), Ethanol ($\text{C}_2\text{H}_6\text{O}$, Alcohol Reagent, anhydrous, denatured, ACS, 94 – 96%, Alfa Aesar), Hexane (C_6H_{14} , ACS, BDH) were used as solvents.

3.2 Characterization

3.2.1 Powder X-ray Diffraction (PXRD)

Powder X-ray Diffraction (PXRD) is vital characterization tool to determine the crystallinity of MOFs crystals. The patterns can be extracted from XRD and give the information such as the unit cell dimensions. By comparing experimental data from XRD with the simulated data from the computational simulation, the phase purity of MOFs can be confirmed.

3.2.2 Scanning Electron Microscopy (SEM)

Scanning Electron Microscopy (SEM) is a crucial tool to obtain a variety of properties from MOFs such as crystal size, morphology, and elemental composition. In order to acquire the high quality of SEM images, the coating of conducting materials (e.g., gold or osmium) on the MOFs is required to decrease charge buildup since the insulating nature of most MOFs. Besides, accelerating voltage of the electron beam is necessary to control in a proper range because the appearances of MOFs crystals can be influenced a lot by accelerating voltage. Even though the higher accelerating voltage can result in more excellent image resolution, the loss of surface detail is inevitable, which means that the surface defects and contamination might be prohibited. In addition, the possibility of local heating increases owing to inelastic electron scattering and local heating might lead to the irreversible damage to MOFs crystals.

3.2.3 Fourier Transform Infrared (FTIR) Spectroscopy

Fourier Transform Infrared (FTIR) Spectroscopy is a tool utilized to obtain an infrared spectrum of absorption or emission of the samples and identify different types of chemical bonds in molecules. It is modern techniques used for qualitative and quantitative analysis. The chemical bonds in a molecule can be determined by analysis of infrared absorption spectrum. Plus, several infrared spectral libraries are accessible to be applied to identify unknown products by comparison to known components in libraries.

3.3 Experiments

3.3.1. α -alumina supports

Porous supports with ~ 22 mm diameter and ~ 2 mm thickness were prepared by the following procedure. Firstly, the 10g of powder and 1 ml of an aqueous PVA binder solution were mixed and ground to ensure the powder was well-mixed. For the preparation of binder solution, the 3 g of polyvinyl alcohol was dissolved in the solution consist of 95 ml of DI water and 5 ml of 1M HNO_3 . 2.1g of the alumina powder was then under 10tons of pressure for 1 minute. For sintering, the alumina disks sat at 1100 $^\circ\text{C}$ for 2 h. The sintered disks were polished with sandpaper (grit#800). In order to remove the particles on the polished side before usage, the disks were immersed in methanol and sonicated for 1 minute. And then, the disks were dried at 120 $^\circ\text{C}$ for 1 h to remove the methanol residue in porous alumina disks.

3.3.2. ZIF-8 seeded supports

2.43 g of zinc nitrate hexahydrate was dissolved in 40 ml of methanol, and 2.59 g of 2-methylimidazole (mIm) linkers and 0.125 g of sodium formate were dissolved in 30 ml of methanol. Dried alumina support was placed vertically with polished side facing down using a Teflon holder and soaked in the metal precursor solution for 1 h. Afterward, the metal-ion-saturated support was inserted in a microwave-resistant glass tube filled with the ligand precursor solution. Microwave irradiation was immediately applied with the power of 100 W for 1.5 min. After cooled down to room temperature, the seeded support was thoroughly rinsed with methanol and kept in 35 ml of fresh methanol for 1 day followed by drying at 60 $^\circ\text{C}$ for 4 h.

3.3.3. ZIF-90 and ZIF-8-90 seeded supports

In order to prepare ZIF-90 and ZIF-8-90 seeded supports, three methods have been implemented, and the preparation of metal and ligand solution are as follow:

3.3.3.1. Synthesis of hybrid ZIF seed crystals depositing on the substrate in methanol³⁰ (MW-S-8-90)

0.48 g of sodium formate, 1.232 g mIm, and 0.865 g of imidazolate-2-carboxaldehyde (ICA) were dissolved in 30 ml of methanol to prepare the ligand solution. For the preparation of metal precursor solution, 4.76g of zinc nitrate hexahydrate was dissolved in 40 ml of methanol.

3.3.3.2. Synthesis of ZIF-90 seed crystals in methanol and DI water³¹ (MW-S-90)

0.816 g of sodium formate and 1.153 g ICA were dissolved in 30 ml of methanol to prepare the ligand solution. For the preparation of metal precursor solution, 2.975 g of zinc nitrate hexahydrate was dissolved in 40 ml of DI water.

3.3.3.3. Synthesis of ZIF-90 seed crystals in DMF and methanol²⁰ (MW-S-90-DMF)

1.153 g ICA were dissolved in 30 ml of DMF to prepare the ligand solution. For the preparation of metal precursor solution, 2.975 g of zinc nitrate hexahydrate was dissolved in 50 ml of methanol.

Bare alumina support was dried thoroughly for 1 h at 120°C and then place vertically (the polished side facing down) with Teflon holder support. Before applying MW (100W, 1.5min) in a glass tube, the alumina supports were soaked into metal precursor solution prepared for at least 1 hr. After MW assisted seeding and cooled down to room temperature, methanol was utilized to clean seeded support, and seeded support was then kept in 35 ml methanol for 24 h along with drying at 60°C for 4hr.

The effect of different concentration of the metal solution (diluted, double, and triple) was explored to optimize the quality of seeded support.

3.3.4. ICA solvent-assisted linker exchange (SALE) on ZIF-8 seeded supports

1.5 g ICA was dissolved in 40 ml methanol at 60 °C for about 6 hours until it is fully dissolved and become the clear solution. ZIF-8 seeded support was placed in linker solution in Teflon container for 12 h at 60 °C. After linker exchange reaction, the seeded support was washing in 35 ml methanol solution for 24 h and dried at room temperature overnight.

3.3.5. Secondary growth of ZIF-90 membranes

Two recipes have been tried for secondary growth of ZIF-90 membranes:

3.3.5.1. Secondary growth with sodium formate

For secondary growth, metal and ligand precursor solutions were prepared by dissolving 0.298 g of zinc nitrate hexahydrate and 0.385 g of ICA in 20 ml of methanol, respectively. The seeded alumina disk was placed vertically using a Teflon holder in a Teflon-lined autoclave. Meanwhile, the metal precursor solution was added to the ligand precursor solution and stirred for 2 min. Then the solution mixture was poured into the Teflon-lined autoclave containing the seeded support. The beaker is then placed in an oven at 90 °C for 4 or 24 h. The resulting membrane was then washed in 35 ml of fresh methanol for 2 days and dried at room temperature for 12 h.

3.3.5.2. Secondary growth without sodium formate

For the preparation of linker solution, 0.384 g of ICA was dissolved in 40ml methanol at 60°C for 4 h until the solution becomes clear and ICA was fully dissolved. And then, 0.296 g of zinc nitrate hexahydrate was added to linker solution and mixed for 2 min to prepare secondary

growth solution. Dried seeded alumina disks were inclined 45° and faced down with the supports of Teflon holder and then soaked in growth solution which was kept in Teflon container. The reactor was then put in 65°C oven for 4 h for secondary growth reaction. After secondary growth, the disk was transferred into another reactor with new growth solution for tertiary growth. After that, the disk with ZIF-90 membrane was placed in a small beaker with fresh 40ml of methanol on the shacking platform for 2 days followed by drying at room temperature for 12 h.

3.3.6. Gas permeation measurement

Binary gas permeation measurements were conducted under 1 bar and room temperature with Wicke-Kallenbach techniques. An equimolar mixture of gas pairs was supplied at total 100 cc/min, and the flow rate of argon sweeping at permeate side was 100 cc/min.

For propylene/propane gas mixture, Gas Chromatography (Agilent GC 7890A equipped with a column of HP-PLOT/Q) was applied to analyze the composition of the outlet from the permeate side of membranes. For the CO_2/CH_4 , H_2/CH_4 , CO_2/N_2 , H_2/CO_2 gas mixtures, the permeate composition was analyzed using a gas analyzer (QGA, Hiden Analytical).

CHAPTER IV

ZIF-90 FILMS AND MEMBRANES FABRICATION

4.1 *In situ* method

In situ method involves the synthesis of membranes in a single step. As reported from Caro's group, well-intergrown ZIF-8 membranes can successfully be built on untreated titania substrates by MW assisted solvothermal approach¹³. In addition, Lai's group was capable of synthesizing ZIF-69 membranes directly on unmodified alumina substrates by direct solvothermal approach.

ZIF-90 membranes growth on bare alumina substrate via simple solvothermal method, however, resulted in poor-intergrown membranes (Figure 11(a) (d)). Only large crystals distributed on alumina substrates due to the unfavorable heterogeneous nucleation on unmodified substrates. In order to promote the heterogeneous nucleation and growth of ZIF-90 membranes, the simple surface modification was applied. This method was inspired by Jeong et al. who grew ZIF-8 films on thermally modified alumina substrates³². They claimed that the firm covalent coordination between alumina substrates and imidazole ligands could form after surface modification and trigger heterogeneous nucleation on the surface of substrates. We came up with two ways to thermally modified alumina substrates: (1) 1.5 min 100W MW heating in ICA solution (2) solvothermal treatment in ICA solution at 60°C for 24 hr. After surface modification, the white alumina substrates became yellowish, and these yellowish alumina substrates were placed into the growth solution for secondary growth. The results were similar to the *in situ*

synthesis on bare alumina substrates as shown in Figure 11. The seeding methods were required to prepare well-intergrown ZIF-90 membranes on porous alumina substrates.

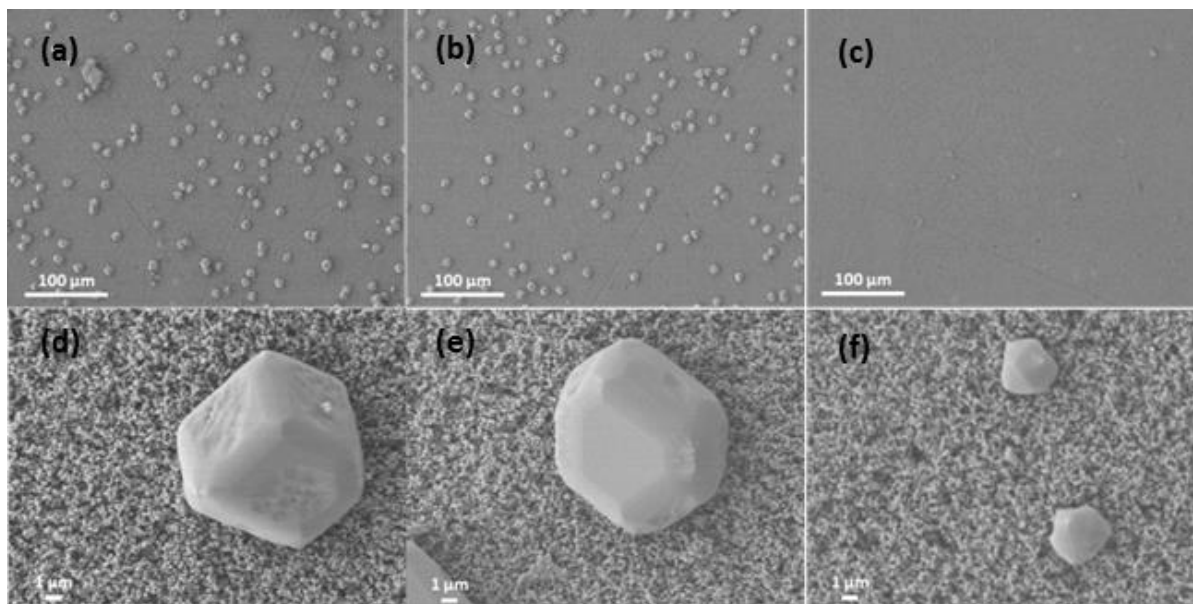


Figure 11. SEM images for (a)(d) in situ growth on a bare alumina substrate (b)(e) modified substrate via MW(1.5 min) in ICA solution (c)(f) amended substrate via solvothermal (60°C, 24hr) process in ICA solution.

4.2 Secondary growth (seeded) method

One significant difficulty to obtain the ZIFs membranes on the substrates is that the bonding between linkers and functional groups on the surface of substrates (e.g., -OH on alumina supports) cannot be provided to form robust and continuous membranes. Moreover, heterogeneous nucleation of MOFs crystals on the substrate is limited and weak. That's why *in situ* method is always challenging. Therefore, chemical modifications¹⁸ and seed coating of the supports²⁰ are usually required to trigger the nucleation and growth of the ZIF-90 layers. Here in, we used the MW-assisted seeding technique to coat seed layers on the supports to prepare well-intergrown ZIF-90 membranes.

Seeding growth (seeded) method is widely accepted to fabricate thin ZIF membranes with better grain boundary structures. The seed crystals layers provide a stronger connection between ZIF membranes and alumina substrates and better heterogeneous nucleation conditions in the growth reaction. High-quality seed crystal layers are comprised of densely-packed nano-sized crystals firmly attached to porous supports with uniform surface coverage. Several techniques are available to coat seed layers on the substrate surface including manual rubbing, dip coating, spin coating, thermal deposition, and MW assisted seeding. MW-assisted seeding is widely used for MOFs membranes synthesis recently and has several advantages: (1) Shorter synthesis time (2) the resulting small seed crystals with uniform size. Herein, we proposed different strategies with MW-assisted seeding method to produce seeded substrates for ZIF-90 membranes growth.

4.2.1 Heteroepitaxial growth on ZIF-8 seeded supports

The MW assisted seeding method in obtaining high-quality ZIF-8 seed crystals coating on the surface of substrates was well-established in our group. High-quality of ZIF-8 seeded alumina substrates can be achieved merely by MW. Since ZIF-90 and ZIF-8 are iso-structure material, heteroepitaxial growth of ZIF-90 membranes on ZIF-8 seeded supports is theoretically possible. Heteroepitaxial growth approach has been investigated in our group before. Jeong and Kwon have successfully grown continuous polycrystalline ZIF-67, another iso-structure of ZIF-8 but with cobalt ion as metal nodes, membranes on ZIF-8 seeded supports.

As shown in Figure 12, the ZIF-90 membranes can be synthesized based on pure ZIF-8 seeded supports through heteroepitaxial growth, but the resulting ZIF-90 membranes showed lots

of roughness and anomalous twin crystals on the surface. The ZIF-90 seeded supports seem necessary to fabricate well-intergrown and well-faceted polycrystalline membranes.

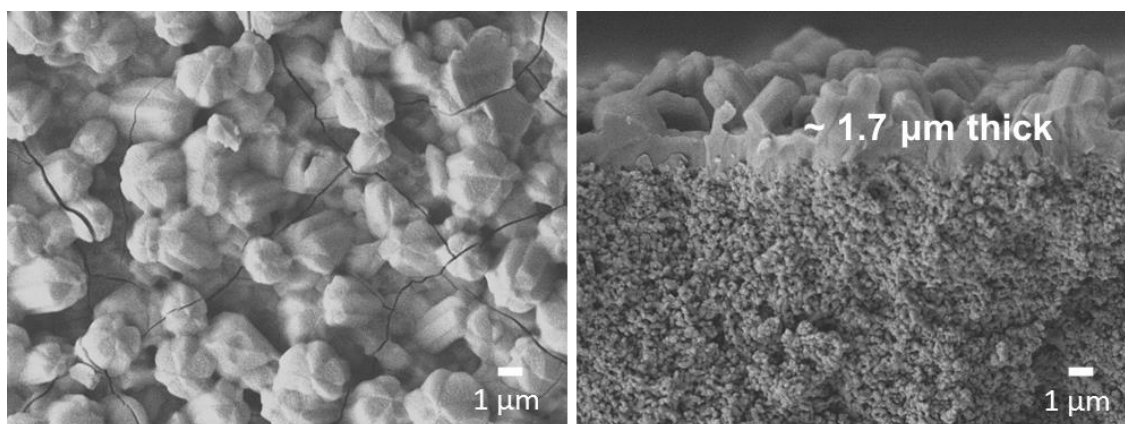


Figure 12 . ZIF-90 membranes growth on ZIF-8 seeded support (a) top view of membranes and (b) cross-section view.

4.2.2 Secondary growth on ZIF-90 seeded supports

4.2.2.1 ZIF-90 and ZIF-8-90 seeded supports

In an attempt to synthesize thin and well-intergrown ZIF-90 membranes, seeded support with densely packed nano-sized seed layers is significant. Four strategies with MW-assisted seeding were proposed to make ZIF-90 seeded supports: (please refer to Experiment section for detailed composition and preparation process)

4. Synthesis of ZIF-90 seeds crystals from ZIF-8 seeded supports modified by ICA linker exchange reaction. (**MW-S-ICA**)
5. Synthesis of hybrid ZIF seed crystals depositing on the substrate in methanol³⁰ (**MW-S-8-90**)
6. Synthesis of ZIF-90 seed crystals in methanol and DI water³¹ (**MW-S-90**)
7. Synthesis of ZIF-90 seed crystals in DMF and methanol²⁰ (**MW-S-90-DMF**)

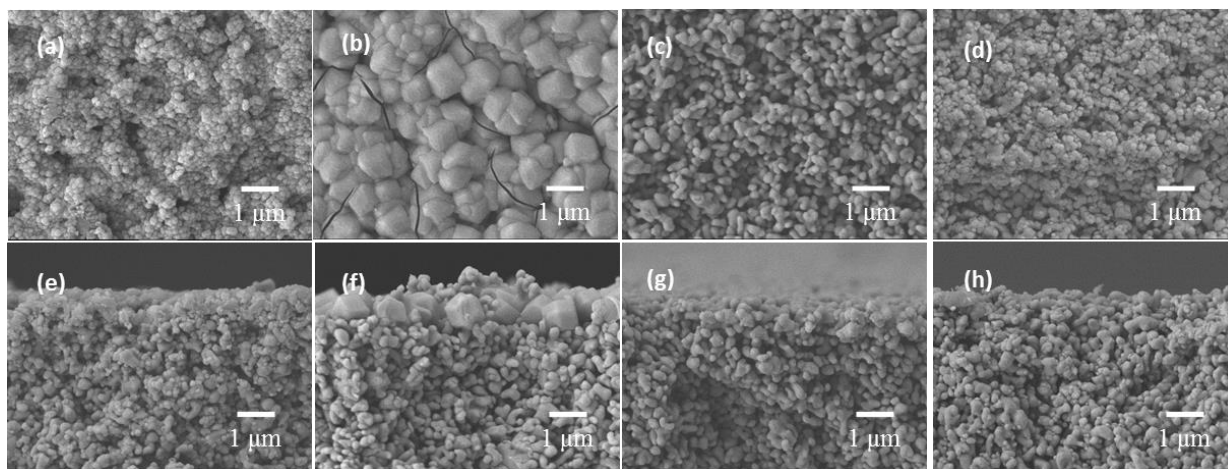


Figure 13. SEM images for ZIF-90 and ZIF-8-90 seeded supports: **MW-S-ICA** (a)Top view (b) cross-section; **MW-S-8-90** (c)Top view (b) cross-section; **MW-S-90** (a)Top view (b) cross-section; **MW-S-90-DMF** (a)Top view (b) cross-section.

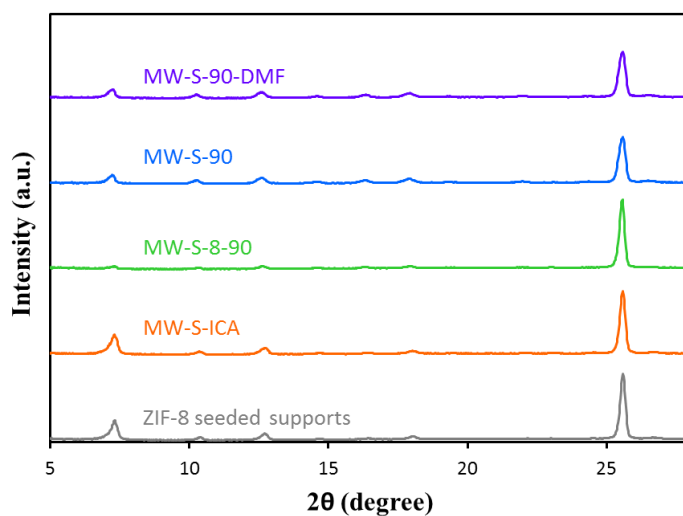


Figure 14. XRD patterns for seeded supports prepared via different strategies.

The resulting ZIF seed layers presented in Figure 13 (a) exhibited well-packed small seeds crystals (~ 200 nm) deposited on the alumina supports. ZIF-8 seed crystals with ZIF-90 linkers incorporated in the frameworks survived after solvent-assisted linker exchange (SALE) reaction. As shown in Figure 13 (b), the seed crystals seem too large (~ 900 nm) and almost

inter-grown with each other. From Figure 13 (c) and (d), the seed crystals can barely be found. However, the XRD pattern (Figure 14) showing the peaks from seed crystals indicated that there are ultramicro-seeds but not visible in such scale. Since that is so, the seeding conditions (**MW-S-8-90**, **MW-S-90**, and **MW-S-90-DMF**) were further optimized by increasing Zn^{2+} concentration by 2 times and 4 times and the outcomes were demonstrated in Figure 16. These results ran counter to our expectation which is that the higher concentration of Zn^{2+} would increase the nucleation rate and form the seed crystals; however, the crystals indeed formed but grew too large and sparsely packed on the alumina supports which conforms to the observation in Zafer et al.'s study³³. They suggested that a decreasing metal/linker ratio results in increasing number of nuclei with the smaller size. Therefore, to increase the number of nano-seeds, decreasing metal/linker ratio – that is, higher linker concentration – is much more efficient. Nonetheless, since the solubility of ICA is limited in methanol, it has the limitation to decrease the ratio of metal/linker to achieve a better quality of seeded supports.

In addition to changing the molar ratio of reactants, double seeding – that is 2 times seeding to the support – was applied to obtain more seed crystals attached to the supports. Even though the double seeding was employed to optimize the MW-S-8-90 and MW-S-90, still, only some large crystals and tiny crystals sparsely packed on the surface of alumina supports shown in Figure 15.

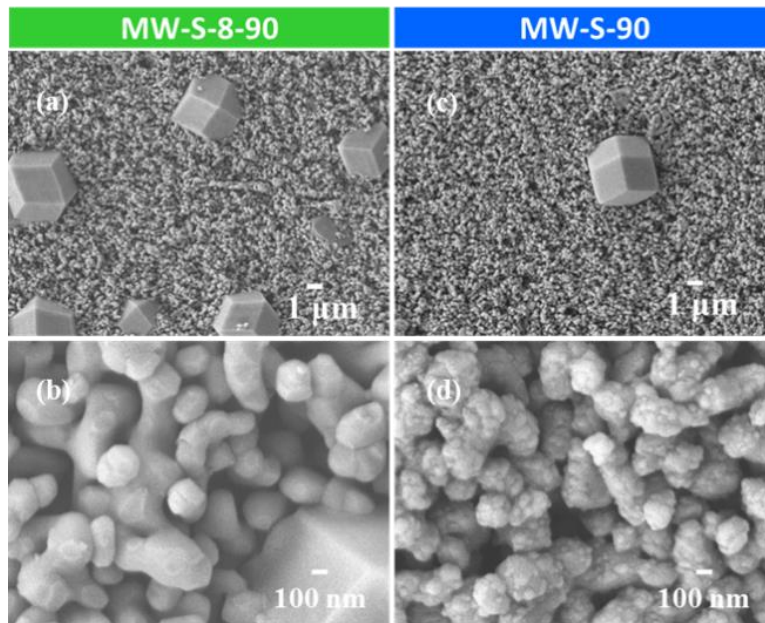


Figure 15. SEM images for double seeded supports via **MW-S-8-90** (a) (b) and **MW-S-90** (c) (d).

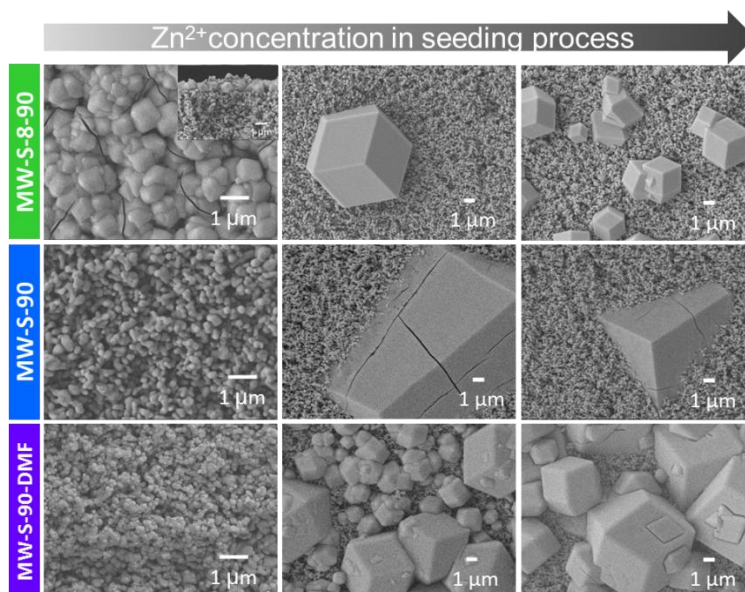


Figure 16. SEM images for seeded supports (**MW-S-8-90**, **MW-S-90**, and **MW-S-90-DMF**) synthesized by different Zn^{2+} concentrations (left: original, middle: double, right: 4 times) in MW seeding.

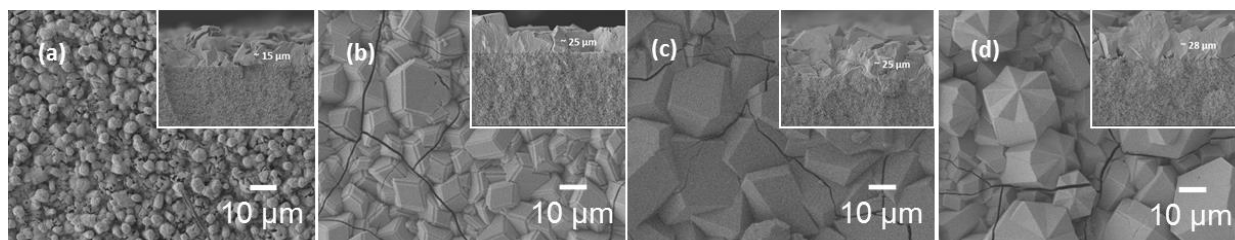


Figure 17. ZIF-90 membranes based on different seeded supports (a) **MW-S-ICA** (b) **MW-S-8-90** (c) **MW-S-90** (d) **MW-S-90-DMF** after secondary growth based on growth solution with sodium formate.

The secondary growth (with sodium formate at 90°C for 24h) was followed based on these seeded supports (synthesized with original concentration of Zn^{2+}), and the results are shown in Figure 17. The well-intergrown ZIF-90 membranes were obtained from each seeded supports. However, ZIF-90 membranes synthesized based on **MW-S-8-90**, **MW-S-90**, **MW-S-90-DMF** seeded supports are too thick ($\sim 20 - 30 \mu m$). Hence, in consideration of the quality of seed layers and the thickness of resulting ZIF-90 membranes, the strategy: making ZIF-8 seeds crystals via MW seeding and apply ICA linker exchange reaction (**MW-S-ICA**) was chosen for further synthesis optimization.

4.2.2.2 Secondary growth on ICA linker exchanged ZIF-8 seeded supports

The first recipe of secondary growth was modified from Caro et al.¹⁸ The growth solution includes linkers, metals, and sodium formate as deprotonator. However, we found out that twin crystals and weird structures tend to form the growth solution including sodium formate as shown in Figure 18.

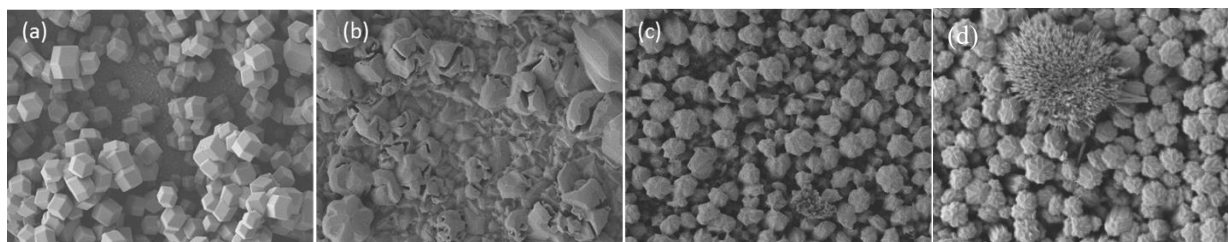


Figure 18. SEM images of ZIF-90 membranes growing (a) without sodium formate at 65°C for 4 h (b) with sodium formate at 65°C for 4 h (c) with sodium formate (2 times concentrated) at 65°C for 4 h (d) with sodium formate (4 times concentrated) at 65°C for 4 h. More defects and weird morphology can be observed after secondary growth with the existence of sodium formate in growth solution.

Therefore, the recipe without sodium formate from Brown et al.²⁰ was applied to synthesize ZIF-90 membranes. In addition to the effect of sodium formate, we also found out that the degree of ZIF-90 linkers incorporated into the ZIF-8 seed frameworks has an impact on the quality of ZIF-90 membranes. Different conditions of ICA concentrations and reaction times for linker exchange reaction have been optimized. The degree of ZIF-90 linker incorporated in ZIF-8 frameworks can be visually determined based on the color and shades as shown in Figure 19. From right to left, the degree of ZIF-90 linker incorporation decreases.

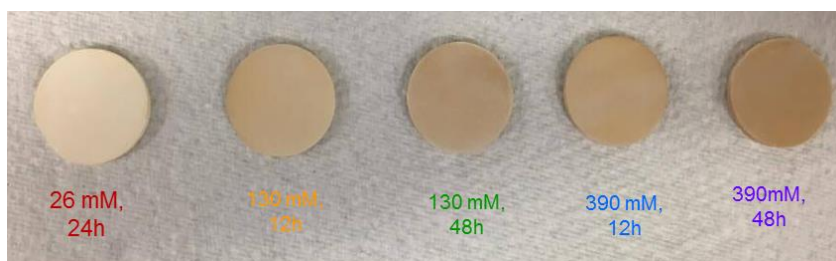


Figure 19. The seeded supports after ICA linker exchange reaction at different reaction time (12, 24,48hr) and concentration of ICA (26mM, 130mM, 390mM).

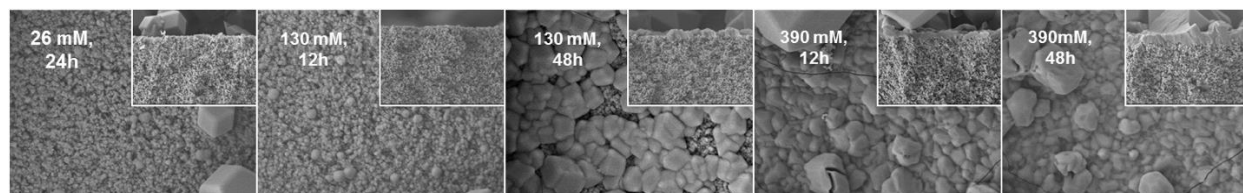


Figure 20. SEM images for ZIF-90 membranes which are synthesized based on seeded supports with ICA linker exchange at different reaction time (12hr, 24hr, 48hr) and concentration of ICA (26mM, 130mM, 390mM).

Figure 20 illustrates the ZIF-90 membranes grew on these seeded supports with different degree of ZIF-90 linker incorporation after secondary growth without sodium formate at 65°C for 4h. Based on the observation, it can be summarized that higher incorporation of ZIF-90 linker in ZIF-8 seed crystals contributed to better intergrown ZIF-90 membranes. In order to achieve more incorporation of ZIF-90 linkers in ZIF-8 seeds, more reaction time and higher ICA concentration are required. The kinetics of solvent assisted linker exchange of ZIF-8 crystal has been studied comprehensively by Nair et al.³⁴ The effect of temperature and reaction time are significant in solvent-assisted linker exchange. For ZIF-8 nanocrystals, near 80% of ZIF-90 linkers can be incorporated in ZIF-8 frameworks after SALE and core-shell morphology can be observed. Although the higher incorporation can be expected in higher temperature, reaction time, and concentration, etching and partial dissolution of crystals could happen in such circumstances and cause morphological defects. Therefore, it is challenging to obtain extremely high incorporation of ZIF-90 in ZIF-8 frameworks and retain the quality of the ZIF-8 crystals. The phenomenon could be supported by the XRD patterns (Figure 21) for ZIF-8 seeded supports after the different degree of ICA linker exchange reaction. The (110) peaks of seed crystals in XRD pattern became lower after linker exchange reaction which means that the dissolving of

seed crystals or defects formation occurred in linker exchange reaction, especially for the one with the highest degree of ZIF-90 linker incorporation.

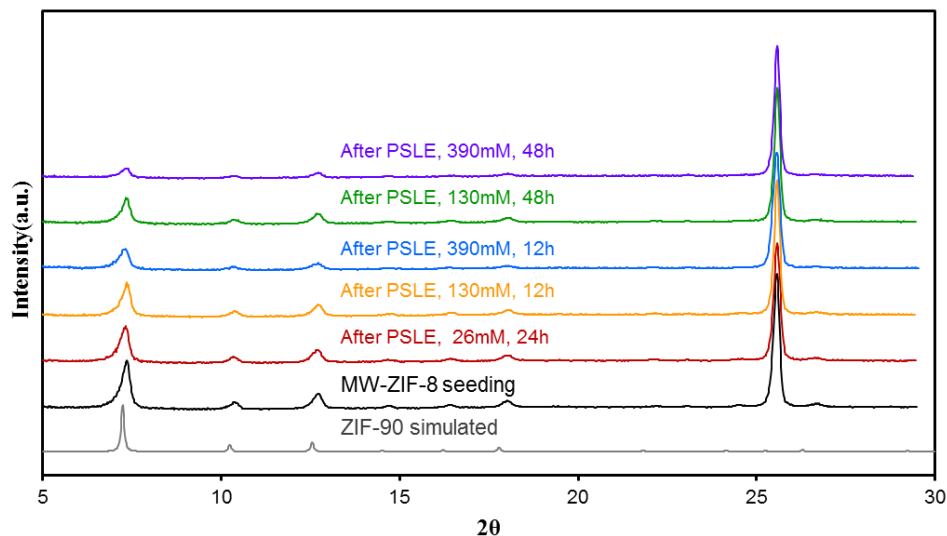


Figure 21. The XRD patterns for ZIF-8 seeded supports and seeded supports after ICA linker exchange reaction with a different time (12h, 24h, 48h), and various ICA concentration (26mM, 130mM, 390mM).

Apart from the incorporation of ZIF-90 linkers, secondary growth reaction time is another factor needed to be optimized. Different growth times were applied, and results are shown in Figure 22. Apparently, the ZIF-90 membrane with 4h growing time (Figure 22 (e) (f)) has the best quality because of inter-growth of the crystals and less large crystals deposited.

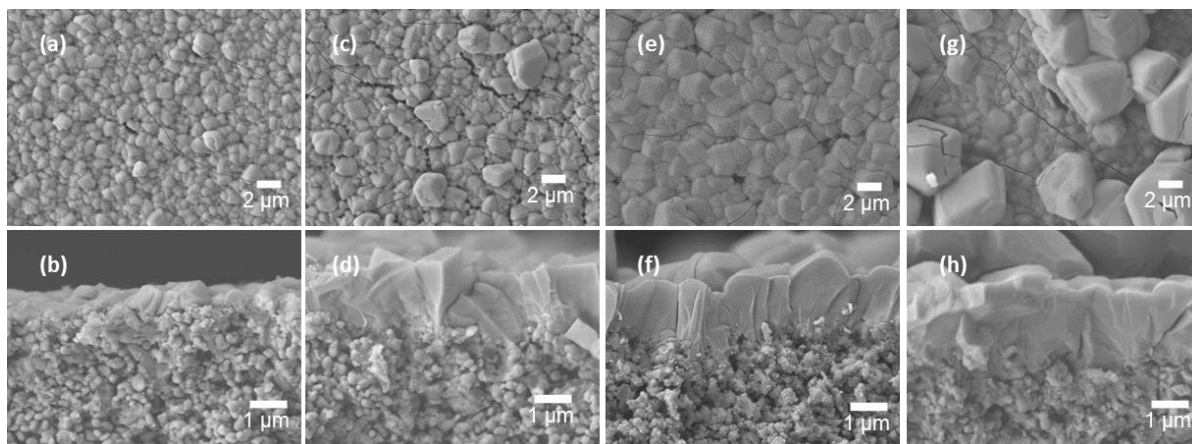


Figure 22. Secondary growth with different growth time. 1hr:(a)(b) 2hr:(c)(d) 4hr:(e)(f) 12hr:(g)(h). The ZIF-90 membranes after 4 hr secondary growth show less roughness and well-intergrown.

Based on the resulting ZIF-90 membranes and crystallinity of seeded supports after linker exchange, the linker exchange reaction in 390mM ICA solution for 12 h at 60°C and 4h secondary growth was selected as an optimized condition to synthesize continuous polycrystalline ZIF-90 membranes.

4.2.3 Tertiary growth on ICA linker exchanged ZIF-8 seeded supports

At the same condition of secondary growth of ZIF-90 membranes, poor-intergrown and well-intergrown ZIF-90 membranes can be obtained at the same time (Figure 23). That is, the reproducibility of ZIF-90 membranes is a severe issue.

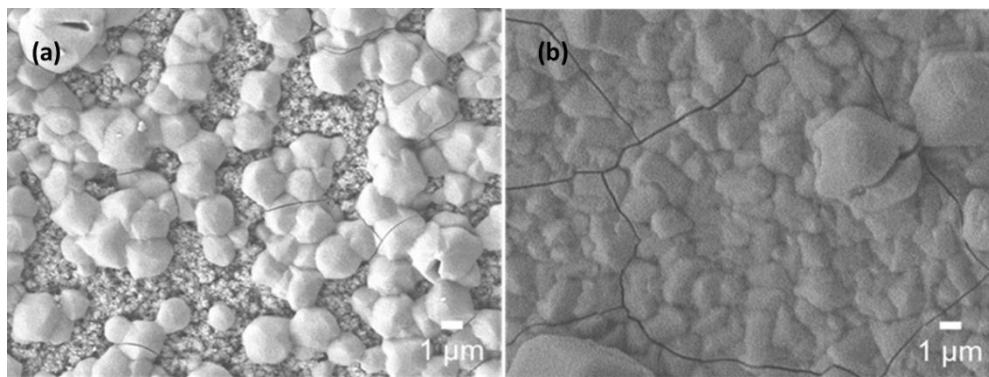


Figure 23. The ZIF-90 membranes under the same synthesis condition (65°C, 4hr) and seeded supports. (a) poor-intergrown ZIF-90 membranes. (b) well-intergrown ZIF-90 membranes.

Tertiary growth method was employed to address this issue. After secondary growth of ZIF-90 membranes, another secondary growth was implemented on the same supports. By doing so, the poor-intergrown crystals can continue growing as continuous polycrystalline ZIF-90 membranes as shown in Figure 25(c) (d) through tertiary growth. Consequently, well-intergrown ZIF-90 membranes can be obtained without reproducibility issues.

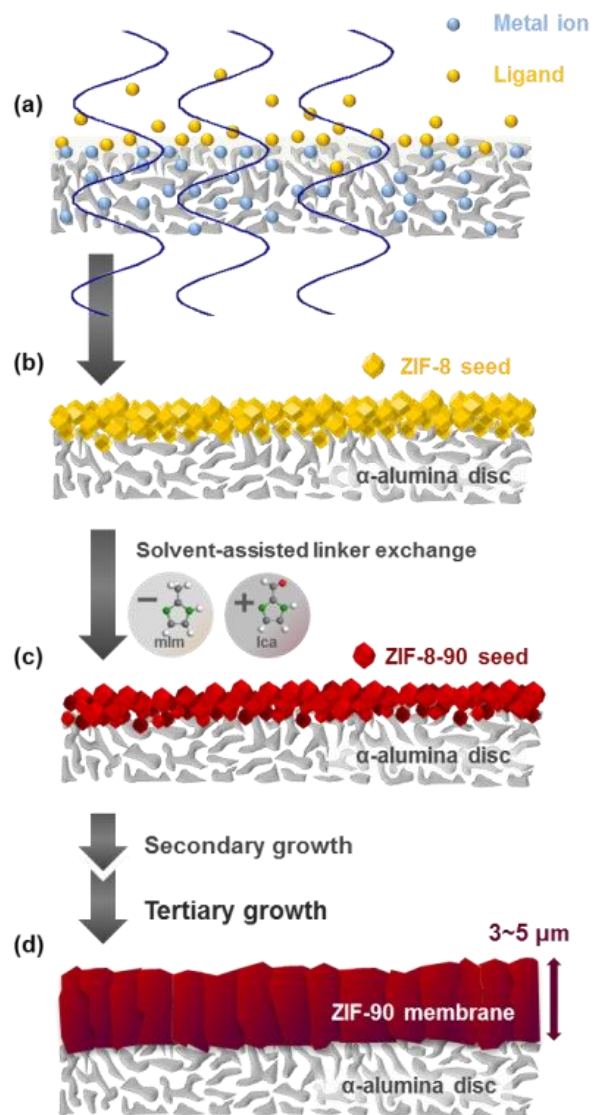


Figure 24. Schematic illustration of the synthesis of ZIF-90 membranes (a) MW-assisted seeding to form ZIF-8 seeds on the porous support (b) ZIF-8 seeded support (c) ZIF-8-90 seeded support after SALE (d) ZIF-90 membrane with thickness $\sim 3 - 5 \mu\text{m}$.

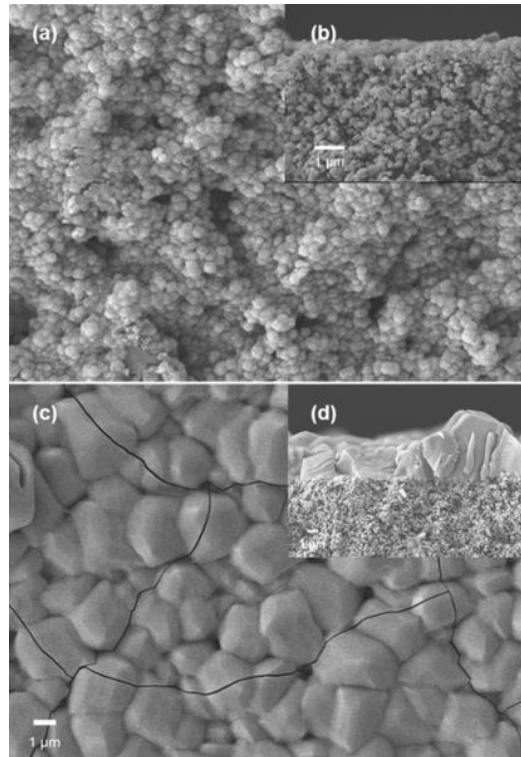


Figure 25. The seeded supports after SALE treatment: (a) Top view, (b) Cross section; ZIF-90 membranes after Tertiary growth: (c) Top view, (d) Cross section.

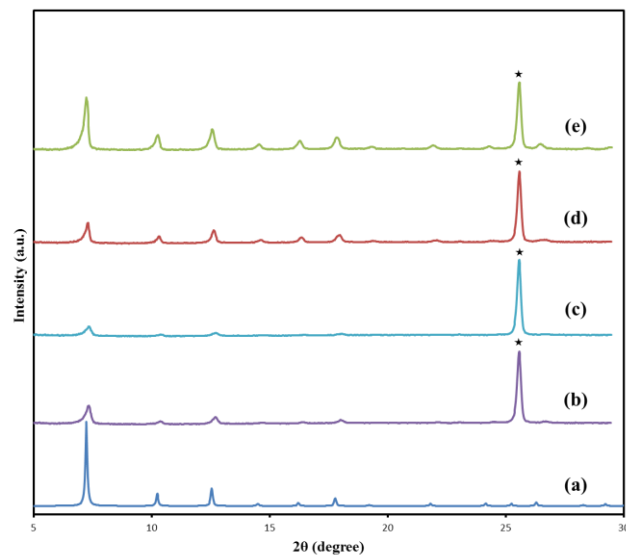


Figure 26. XRD pattern (a)ZIF-90 simulated (b)ZIF-8 seeded support (c)ZIF-8 seeded supports after SALE (d)ZIF-90 membrane synthesized via secondary growth (e)ZIF-90 membrane synthesized via tertiary growth (★) Al_2O_3 supports.

CHAPTER V

ELIMINATION OF CRACKS ON ZIF-90 MEMBRANES

5.1 The crack formation

The crack formation could be observed in the ZIF-90 membranes after tertiary growth. The cracks in the membranes would likely ruin the performance of gas separation. Hence, to eliminate the crack formation is indispensable to obtain ZIF-90 membranes for gas separation applications.

The crack formation could be attributed to the pressure gradient between the dried surface and wet part of the membrane, which leads to differential shrinkage of the frameworks. The low permeability of the membranes causes a pressure gradient. That results in the tension near the drying surface and contraction of the networks. This difference in shrinkage contributed to the drying stress and crack formation.

The greatest tension occur at drying surface could be simplified as²²:

$$\delta_x(L) \approx L \eta_L \dot{V}_E / 3D \quad (15)$$

L = thickness

η_L = viscosity of liquid

\dot{V}_E = rate of evaporation

D = permeability of the networks

Therefore, saturated drying to reduce the evaporation rate could be an effective strategy to eliminate crack formation induced by drying stress.

The surface tension at liquid/solid interface in pores of frameworks and vapor pressure gradient at the liquid/gas interface in different pores in the membranes during drying could give rise to the crack formation induced by capillary force. When drying, the larger pore would dry faster than small pores because vapor pressure at the liquid/gas interface is inversely proportional to the radius of curvature. The higher tension in small pores generates the asymmetric stress that cracks the frameworks at non-uniformity pore structure such as grain boundary or defects²¹.

5.2 Approaches to reduce crack formation

5.2.1 Saturated drying

Saturated drying, which is drying in nearly saturated conditions, can efficiently decrease the drying rate and reduce the tensile stress on the surface which would lead to crack formation. Saturated drying has been used to eliminate the cracks in the fabrication of ZIF-78 membranes²⁴. Unfortunately, the cracks still exist on the ZIF-90 membranes after saturated drying with methanol (Figure 27 (h)). The drying rate of saturated condition might not be enough to obliterate the crack formation. Therefore, we decided to use a less volatile solvent such as DMF and ethanol to decrease the drying rate further to reduce the crack formation.

5.2.2 Saturated drying with less volatile solvent (DMF, Ethanol)

Even though some etching and cracks formation observed after saturated drying with ethanol (Figure 27 (e)), the density of cracks on the ZIF-90 membranes reduced in comparison with the one with methanol. More promising results were obtained in the case of saturated drying with DMF with is much less volatile solvent than methanol depending boiling point. Despite some bump lines were formed, the cracks are almost eliminated after saturated drying with DMF for 5 days at 40°C (Figure 27 (b)).

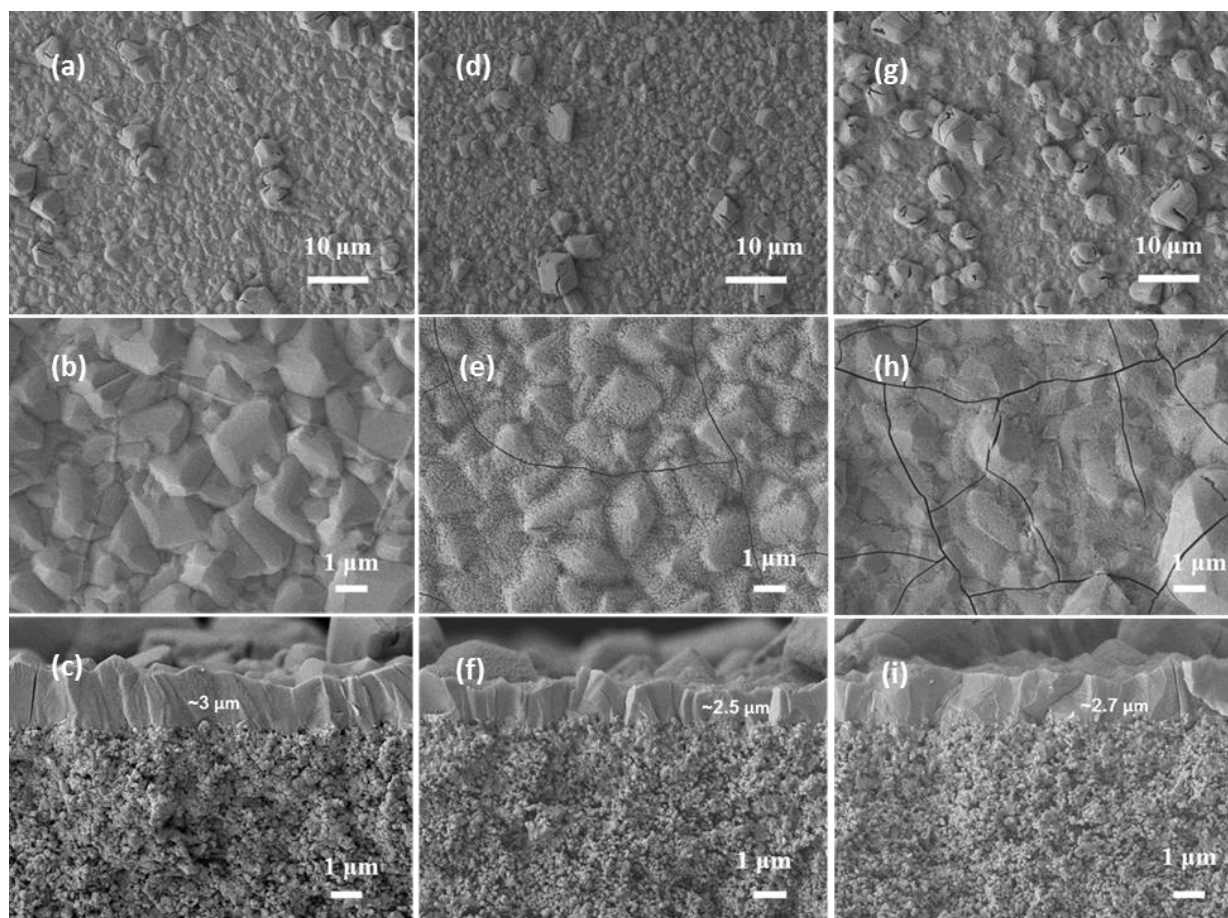


Figure 27. The ZIF-90 membranes after saturated drying with DMF : (a)(b)top view(c)cross-section view; Ethanol: (d)(e)top view(f)cross-section view; Methanol: (g)(h)top view(i)cross-section view.

5.2.3 Others

In addition to saturated drying, an additive such as a surfactant to reduce the capillary force might be another useful strategy to adopt. Jeong et al. have proposed the strategy to apply surfactant to reduce the capillary force and crack formation after drying. Therefore, further study to use surfactant was included in future works to reduce the cracks on ZIF-90 membranes further. Moreover, CO₂ supercritical drying could be the ultimate and most efficient way to eliminate the capillary force which could likely lead to crack formation. However, CO₂

supercritical drying is quite complicated and expensive. This approach should not be considered to produce ZIF-90 membranes for gas separation.

CHAPTER VI

CONCLUSION AND FUTURE WORKS

6.1 Conclusion

In summary, this work demonstrates that ZIF-90 membranes can be fabricated by MW-assisted seeding of ZIF-8, ICA solvent-assisted linker exchange, and tertiary growth of ZIF-90 membranes, with complete surface coverage and but still with minor thin cracks. Moreover, the thickness of ZIF-90 membrane is only ~ 3 to $5 \mu\text{m}$ which is 4 times thinner than the ones synthesized on chemically modified alumina supports¹⁸. This work gives an alternative to synthesize ZIF-90 membranes without complex chemical modification of α -alumina supports. Further study for hydrocarbon separation would be complete in the future after the gas permeation measurement is set up.

6.2 Future works

6.2.1 Effective way to eliminate the cracks and gas permeation measurements of C4 hydrocarbons for defect-free ZIF-90 membranes

Binary gas permeation data for H_2 , CO_2 , N_2 , CH_4 , C_3H_6 , and C_3H_8 have been collected at room temperature. Permeation as a function of the size of gas molecular was shown in Figure 28. The gases show a strong trend of decreasing permeance with increasing kinetic diameter, indicating that the permeation properties are mainly influenced by transports through ZIF-90 pores rather than the defects such as thin cracks. The CO_2/CH_4 and $\text{CO}_2/\text{C}_3\text{H}_8$ selective factors are ~ 1.3 and ~ 0.84 which is well above the Knudsen selectivities 0.8 and 0.6. Further targeted C4

hydrocarbon permeation and separation performance measurement would be conducted in the future. Moreover, the further study and trials of the elimination of cracks on the membranes are required to achieve high-quality ZIF-90 membranes and excellent gas separation performance.

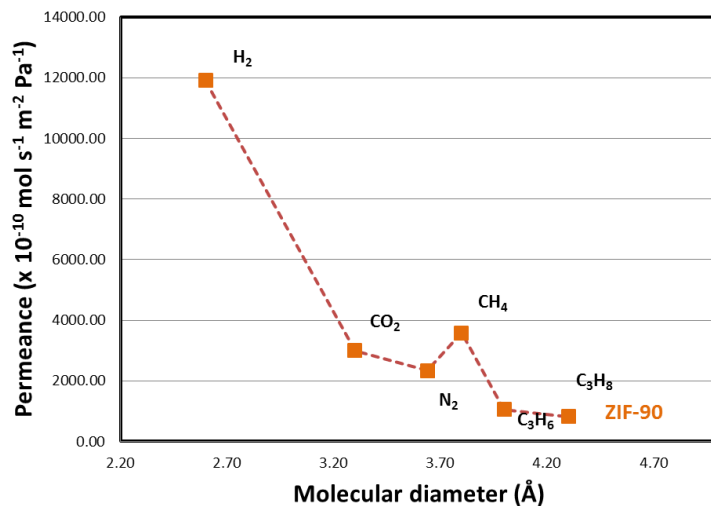


Figure 28. Permeance as a function of the size of gas molecular.

6.2.2 Using polymeric hollow fibers as substrates

In our group, the microfluidic approach has been utilized to synthesize ZIF-8 membranes on bore side of polymeric hollow fibers. Compared to ceramic supports, polymeric supports would be cheaper and more accessible. In addition, hollow fiber can offer large area per volume for gas separation which can enhance the productivity of process so that more profit can be generated. Based on the former experience of synthesis ZIF-8 membranes on polymeric hollow fibers, ZIF-90 membranes are hopeful to be synthesized on polymeric hollow fiber and achieve better performance for gas separation in industry.

6.2.3 Post-synthetic modifications by linker exchange

Post-synthetic modification via covalent chemistry on organic linkers in the ZIF-90 frameworks has been well studied. However, post-synthetic linker exchange modification remains to be discovered. In our group, we already investigated ICA (ZIF-90 linkers) exchange reaction with linkers in polycrystalline ZIF-8 membranes on alumina disks and found out that the permeance of propylene improved but the selectivity of propylene/propane separation retained because the effective thickness reduced. Furthermore, the preliminary results showed that linker exchange could occur between ICA linkers in ZIF-90 crystal powder and mIm (ZIF-8) linkers in solution. Hence, it is worthy to studying linkers exchange on polycrystalline ZIF-90 membranes. Eventually, since ZIF-8 structures have smaller aperture size $\sim 4.0\text{\AA}$ than ZIF-90 effective aperture size $\sim 5\text{\AA}$, we expected that the film formed by incorporation of ZIF-8 linkers on the surface of ZIF-90 membrane could provide ultra-thin selective ZIF-8 membrane and further enhance the performance for gas separation such as propylene/propane.

REFERENCES

1. Zhang, C. *et al.* Unexpected molecular sieving properties of zeolitic imidazolate framework-8. *J. Phys. Chem. Lett.* **3**, 2130–2134 (2012).
2. Gehre, M., Guo, Z., Rothenberg, G. & Tanase, S. Sustainable Separations of C4-Hydrocarbons by Using Microporous Materials. *ChemSusChem* **10**, 3947–3963 (2017).
3. Recent Progress on Metal-Organic Framework Membranes for Gas Separations: Conventional Synthesis vs. Microwave-Assisted Synthesis. *Membr. J.* **27**, 1–42 (2017).
4. Baker, R. W. Future Directions of Membrane Gas Separation Technology. *Ind. Eng. Chem. Res.* **41**, 1393–1411 (2002).
5. Baker, R. W. & Lokhandwala, K. Natural Gas Processing with Membranes: An Overview. *Ind. Eng. Chem. Res.* **47**, 2109–2121 (2008).
6. none. Materials for Separation Technologies. Energy and Emission Reduction Opportunities. (2005). doi:10.2172/1218755
7. Bird, A. J. & Trimm, D. L. Carbon molecular sieves used in gas separation membranes. *Carbon* **21**, 177–180 (1983).
8. Fuertes, A. B. & Menendez, I. Separation of hydrocarbon gas mixtures using phenolic resin-based carbon membranes. *Sep. Purif. Technol.* **28**, 29–41 (2002).
9. Wang, Q., Wu, A., Zhong, S., Wang, B. & Zhou, R. Highly (h0h)-oriented silicalite-1 membranes for butane isomer separation. *J. Membr. Sci.* **540**, 50–59 (2017).
10. Eum, K. *et al.* Highly Tunable Molecular Sieving and Adsorption Properties of Mixed-Linker Zeolitic Imidazolate Frameworks. *J. Am. Chem. Soc.* **137**, 4191–4197 (2015).

11. Ismail, A. F., Khulbe, K. C. & Matsuura, T. *Gas Separation Membranes : Polymeric and Inorganic*. (Springer, 2015).
12. Wijmans, J. G. & Baker, R. W. The solution-diffusion model: a review. *J. Membr. Sci.* **107**, 1–21 (1995).
13. Bux, H. *et al.* Zeolitic imidazolate framework membrane with molecular sieving properties by microwave-assisted solvothermal synthesis. *J. Am. Chem. Soc.* **131**, 16000–16001 (2009).
14. Liu, Y., Hu, E., Khan, E. A. & Lai, Z. Synthesis and characterization of ZIF-69 membranes and separation for CO₂/CO mixture. *J. Membr. Sci.* **353**, 36–40 (2010).
15. Li, Y.-S. *et al.* Controllable Synthesis of Metal-Organic Frameworks: From MOF Nanorods to Oriented MOF Membranes. *Adv. Mater.* **22**, 3322–3326 (2010).
16. Kwon, H. T. & Jeong, H.-K. *In Situ* Synthesis of Thin Zeolitic–Imidazolate Framework ZIF-8 Membranes Exhibiting Exceptionally High Propylene/Propane Separation. *J. Am. Chem. Soc.* **135**, 10763–10768 (2013).
17. Hillman, F., Brito, J. & Jeong, H.-K. Rapid One-Pot Microwave Synthesis of Mixed-Linker Hybrid Zeolitic-Imidazolate Framework Membranes for Tunable Gas Separations. *ACS Appl. Mater. Interfaces* (2018). doi:10.1021/acsami.7b18506
18. Huang, A., Dou, W. & Caro, J. Steam-Stable Zeolitic Imidazolate Framework ZIF-90 Membrane with Hydrogen Selectivity through Covalent Functionalization. *J. Am. Chem. Soc.* **132**, 15562–15564 (2010).
19. Kwon, H. T. & Jeong, H.-K. Highly propylene-selective supported zeolite-imidazolate framework (ZIF-8) membranes synthesized by rapid microwave-assisted seeding and secondary growth. *Chem. Commun.* **49**, 3854 (2013).

20. Brown, A. J. *et al.* Continuous Polycrystalline Zeolitic Imidazolate Framework-90 Membranes on Polymeric Hollow Fibers. *Angew. Chem. Int. Ed.* **51**, 10615–10618 (2012).
21. Shah, M., McCarthy, M. C., Sachdeva, S., Lee, A. K. & Jeong, H.-K. Current Status of Metal–Organic Framework Membranes for Gas Separations: Promises and Challenges. *Ind. Eng. Chem. Res.* **51**, 2179–2199 (2012).
22. Brinker, C. J. & Scherer, G. W. *Sol-Gel Science: The Physics and Chemistry of Sol-Gel Processing*. (Elsevier Science, 2013).
23. Yoo, Y., Varela-Guerrero, V. & Jeong, H.-K. Isorecticular Metal–Organic Frameworks and Their Membranes with Enhanced Crack Resistance and Moisture Stability by Surfactant-Assisted Drying. *Langmuir* **27**, 2652–2657 (2011).
24. Dong, X. *et al.* Synthesis of zeolitic imidazolate framework-78 molecular-sieve membrane: defect formation and elimination. *J. Mater. Chem.* **22**, 19222 (2012).
25. Tsapatsis, M. Toward High-Throughput Zeolite Membranes. *Science* **334**, 767–768 (2011).
26. Lee, M. J., Kwon, H. T. & Jeong, H.-K. High-Flux Zeolitic Imidazolate Framework Membranes for Propylene/Propane Separation by Postsynthetic Linker Exchange. *Angew. Chem. Int. Ed.* **57**, 156–161 (2018).
27. Hu, Y. *et al.* Zeolitic Imidazolate Framework/Graphene Oxide Hybrid Nanosheets as Seeds for the Growth of Ultrathin Molecular Sieving Membranes. *Angew. Chem. Int. Ed.* **55**, 2048–2052 (2016).
28. Hou, J., Sutrisna, P. D., Zhang, Y. & Chen, V. Formation of Ultrathin, Continuous Metal–Organic Framework Membranes on Flexible Polymer Substrates. *Angew. Chem.* **128**, 4015–4019 (2016).

29. Shamsaei, E. *et al.* Rapid synthesis of ultrathin, defect-free ZIF-8 membranes via chemical vapour modification of a polymeric support. *Chem. Commun.* **51**, 11474–11477 (2015).
30. Cravillon, J. *et al.* Rapid Room-Temperature Synthesis and Characterization of Nanocrystals of a Prototypical Zeolitic Imidazolate Framework. *Chem. Mater.* **21**, 1410–1412 (2009).
31. Thompson, J. A. *et al.* Hybrid Zeolitic Imidazolate Frameworks: Controlling Framework Porosity and Functionality by Mixed-Linker Synthesis. *Chem. Mater.* **24**, 1930–1936 (2012).
32. McCarthy, M. C., Varela-Guerrero, V., Barnett, G. V. & Jeong, H.-K. Synthesis of Zeolitic Imidazolate Framework Films and Membranes with Controlled Microstructures. *Langmuir* **26**, 14636–14641 (2010).
33. Öztürk, Z., Filez, M. & Weckhuysen, B. M. Decoding Nucleation and Growth of Zeolitic Imidazolate Framework Thin Films with Atomic Force Microscopy and Vibrational Spectroscopy. *Chem. – Eur. J.* **23**, 10915–10924 (2017).
34. Jayachandrababu, K. C., Sholl, D. S. & Nair, S. Structural and Mechanistic Differences in Mixed-Linker Zeolitic Imidazolate Framework Synthesis by Solvent Assisted Linker Exchange and *de Novo* Routes. *J. Am. Chem. Soc.* **139**, 5906–5915 (2017).